SAND2019-XXXXX

SAND2019-2573PE

Structure-property Relationships in Nanoporous Inorganic Frameworks: How the Pore Determines the Bulk Scale Energy & Environmental Applications

Tina M. Nenoff,*

*Senior Scientist
Materials, Chemistry and Physics Center
Sandia National Laboratories
Albuquerque, NM USA
tmnenof@sandia.gov

This work was supported as part of the Center for Understanding and Control of Acid Gas-Induced Evolution of Materials for Energy (UNCAGE-ME), an Energy Frontier Research Center, funded by the U.S. Department of Energy (DOE), Office of Science, Office of Basic Energy Sciences (BES) under Award DE-SC0012577.
Sandia National Laboratories is a multimission laboratory managed and operated by National Technology and Engineering Solutions, LLC., a wholly owned subsidiary of Honeywell International, Inc., for the U.S. Department of Energy's National Nuclear Security Administration under contract DE-NA-0003525.

Technical Focus

- Technical Focus:
  Chemical study of confinement and reactivity of ions and molecules
  in micro- and nano-porous materials
  - zeolites, metal-organic frameworks (MOFs), clays and amorphous silicas

- The study of Structure-Property Relationships on the nanoscale enabling the informed testing of the materials for a wide range of interests.

- Structure analysis of host-guest systems on the nanoscale has led to strong collaborations with staff scientists at the APS for synchrotron data collection & Pair Distribution Function (PDF) analysis

- Strong Interdisciplinary Teams working in concert.
  diverse programs require diverse teams
  chemists, engineers, computational modelers
  national labs, universities and industry

- Mentoring: postdocs, young staff and collaborating young professors,
  strong support of women and minorities into the sciences

Program Development & Management - Nenoff

- R&D portfolio divided into five general topic areas:
  - High selectivity rad ion & capture nanoporous materials
  - Supported Nanoparticles
  - Gas separations nanoporous materials & membranes
  - Photoluminescence MOFs
  - TQM oxides and chalcogenides

- Developed strong relationships at DOE, resulted in *long running* programs
  - DOE/Office of Science/EFRC *UNCAGE-ME* (PI: Krista Walton)
  - DOE/NA115 (Aging and Lifetime)
  - DOE/EERE/AMO, H_2, EM
  - DOE/Office of Nuclear Energy

- Research Group works in *TRL 1 - 9*

- PI: 2 different multiyear, multimillion $ CRADAs
  - SNL, BP, Temec, Coors Ceramics, University Cincinnati:
    Zeolite Membranes for HC isomer feedstock purification
  - SNL, Goodyear Chemicals, University Cincinnati:
    Membranes for Separations of High Volume $C_4/C_5/C_6$ Mixtures

R&D Area 1: Novel nanoporous materials for Rad Ion & Gas Separations and Storage

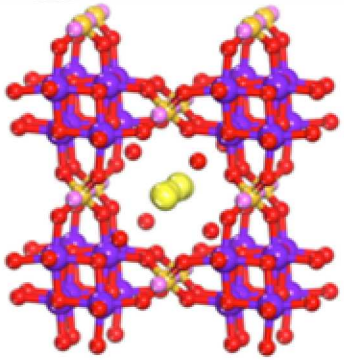

R&D100 1996
JACerS, 2009, *92(9)*, 2144
JACerS, 2011, *94(9)*, 3053
Solvent Extr. & Ion Exch, 2012, *30*, 33

CST, Cs^+ removal from water to Pollucite Waste Form
US Patents *6,479,427; 6,110,378*

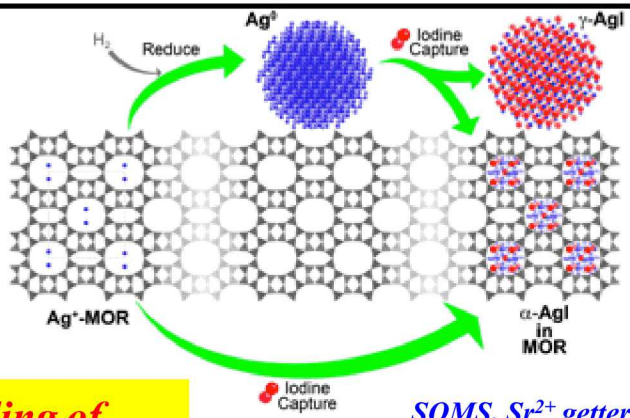

Ag-MOR I_2(g) capture & mechanisms
JACS, 2010, *132*(26), 8897
J Phys Chem Lett, 2011, *2*,2742
I&ECR 2017, *56*(8), 2331

Fundamental understanding of what controls ion or gas selectivity, through structure-property relationship studies

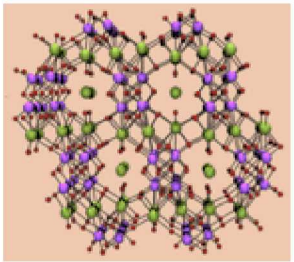

SOMS, Sr^{2+} getter, 1-step to Perovksite WF
JACS, 2002,*124(3)*, 1704
US Patent *7,122,164*

I_2/ZIF-8, Isolation to Waste Form
JACS, 2011,*133(32)*,12398
US Patent filed 2012
JACS 2013, *135*, 16256

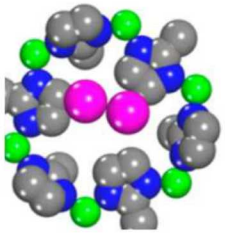

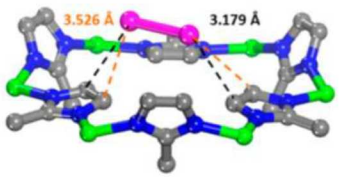

MOF Amorphization for Gas Storage
JACS, 2011,*133*(46),18583
US Patent 9,552,897; 2017

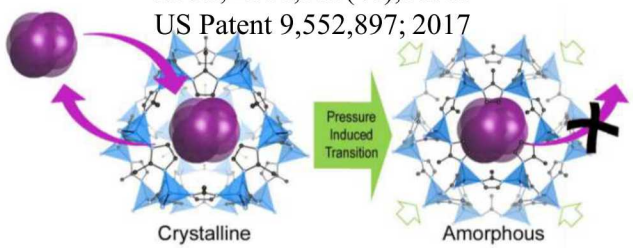

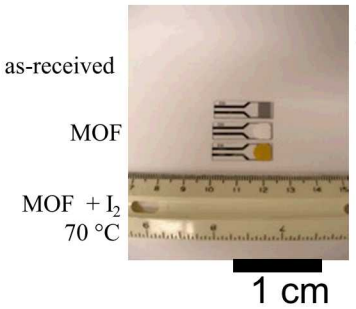

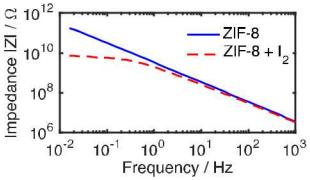

I_2 Gas Sensor
ACS Appl. Mater. Interfaces, **2017**,*9*,44649

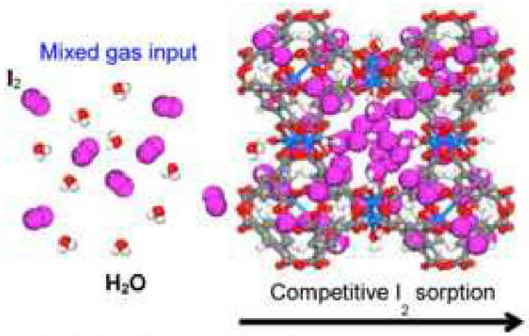

Cu-BTC: I_2 from Humid Gas Stream
Chem. Mater. 2013, *25*(13), 2591

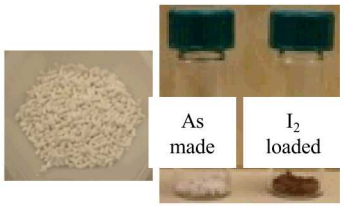

Binder Free MOF Pelletization
US Patent 2015 *9,117,560*

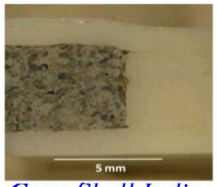

Universal Core-Shell Iodine Glass Waste Form & Getter
JACerS, 2011, *94*(8), 2412
US Patent 8,262,950; 2012

Ion Exchange Selectivity: Why?

Ion selectivity is dictated by a variety of factors including:
surface adsorption, structural/geometry, sphere of hydration energetics: **What is role of Water?**

SOMS: $Na_2Nb_{2-x}M_xO_{6-x}(OH)_x \cdot H_2O$

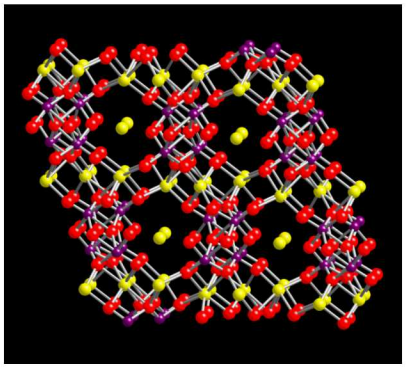

Clinoptilolite/Heulandite:
$[X]_{4-6}[Al_6(Al,Si)_4Si_{26}O_{72}] \cdot xH_2O$

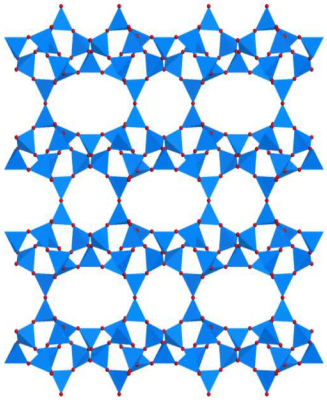

Montmorillonite Clays substitutions of tetra/oct sites affect interlayer hydrated ions

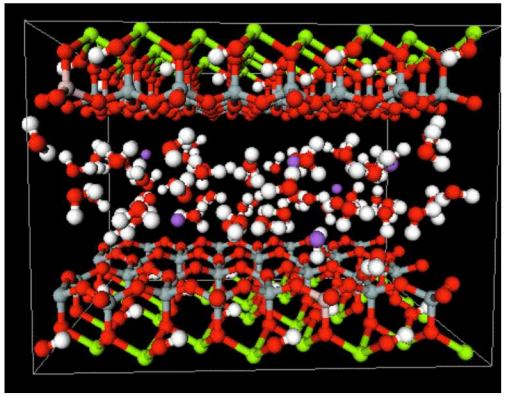

Sepiolite:
$Mg_8Si_{12}O_{30}(OH)_4 \cdot 12H_2O$

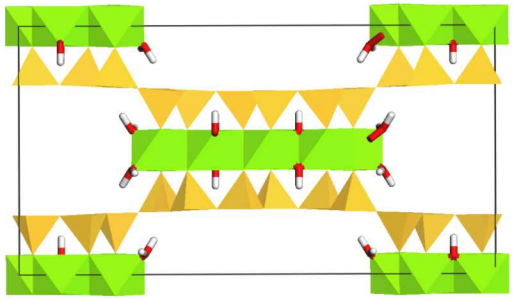

Palygorskite:
$Mg_5Si_8O_{20}(OH)_2 \cdot 8H_2O$

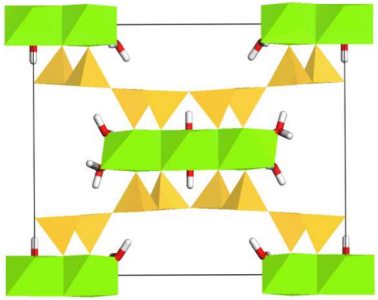

J. Phys. Chem.C, **2007,** *111*(35), 13212
PCCP, **2008**, *10*, 800
J. Phys. Chem. C., **2008,** *112,* 13629
J. Am. Chem. Soc., **2009**, *131*(23), 8155
J. Phys. Chem. C, **2015**, 119, 28005

Framework-Ion-Water Behavior

$Cs^{+} < Rb^{+} < Ba^{2+} < K^{+} < Sr^{2+} < Na^{+} < Ca^{2+} < Li^{+} < Mg^{2+}$

Lowest Hydration Energy

Highest Hydration Energy

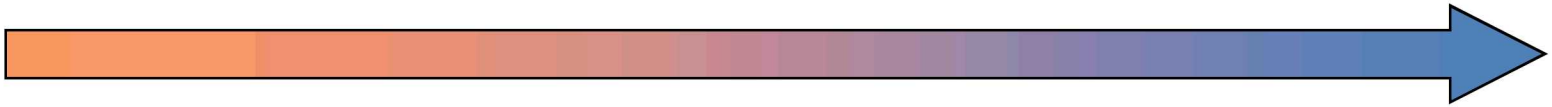

Weakly Hydrated

Strongly Hydrated

Framework-Ion Interactions Dominate

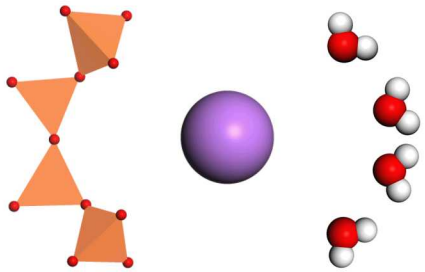

Water-Ion Interactions Dominate

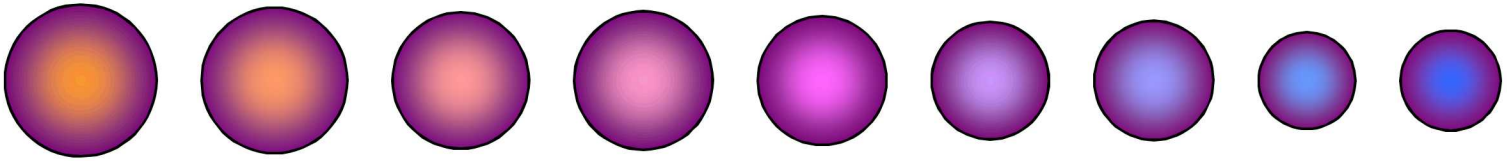

Largest Ionic Radius

Smallest ionic Radius

Methods for exploring the Ion-Framework, Ion-Water, Framework- Water interactions include:

Characterization: Inelastic Neutron Scattering, NMR

Modeling: DFT, MD Simulations (Force Field calculations, LAAMPS) and Power Spectra

Los Alamos Neutron Science Center (LANSCE)

Inelastic Neutron Scattering (INS) Experiment

Linear accelerator with protons accelerated to 0.84 *c* and impacting tungsten target to generate neutrons

Filter Difference Spectrometer

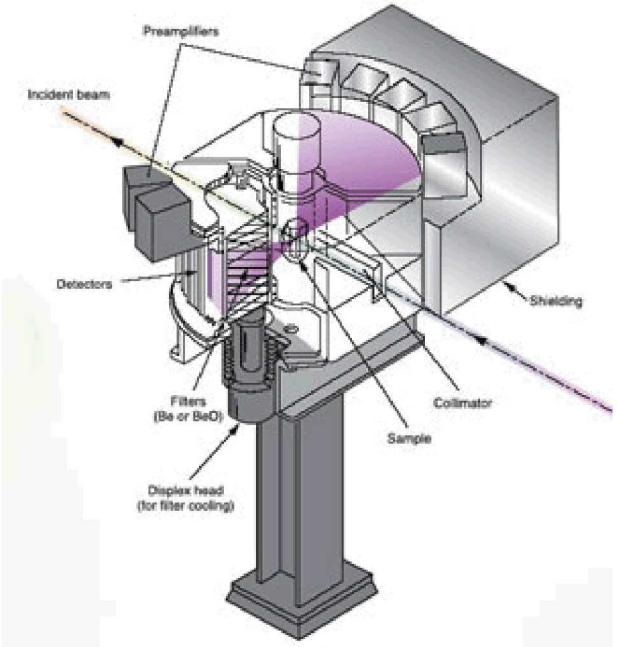

- Detectors have high sensitivity to scattering of neutrons by sample
- Special sensitivity to hydrogen-containing molecules
- Obtain vibrational spectra by neutron energy loss using Be filters and TOF analysis

Water Molecular Libration Modes

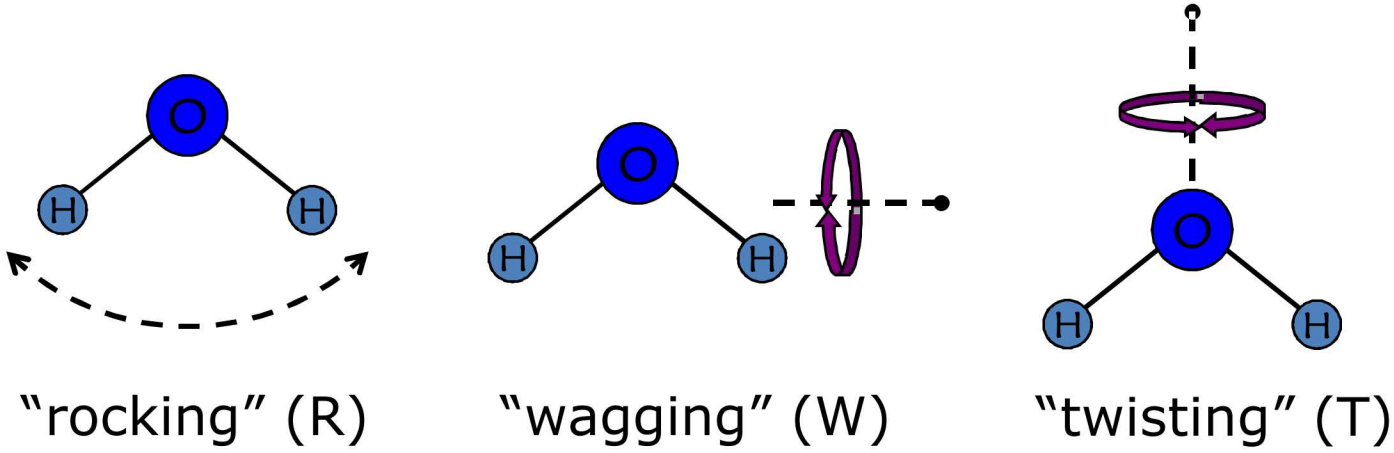

"rocking" (R) "wagging" (W) "twisting" (T)

- Typically centered around ~500 cm^{-1}
- Extremely sensitive to environment. (H-bonding, ion coordination, sterics)
- Intensity decreases and strong broadening with H_2O disorder (multiple configurations) and gives rise to Librational Edge

Inelastic Neutron Scattering (INS) of Water

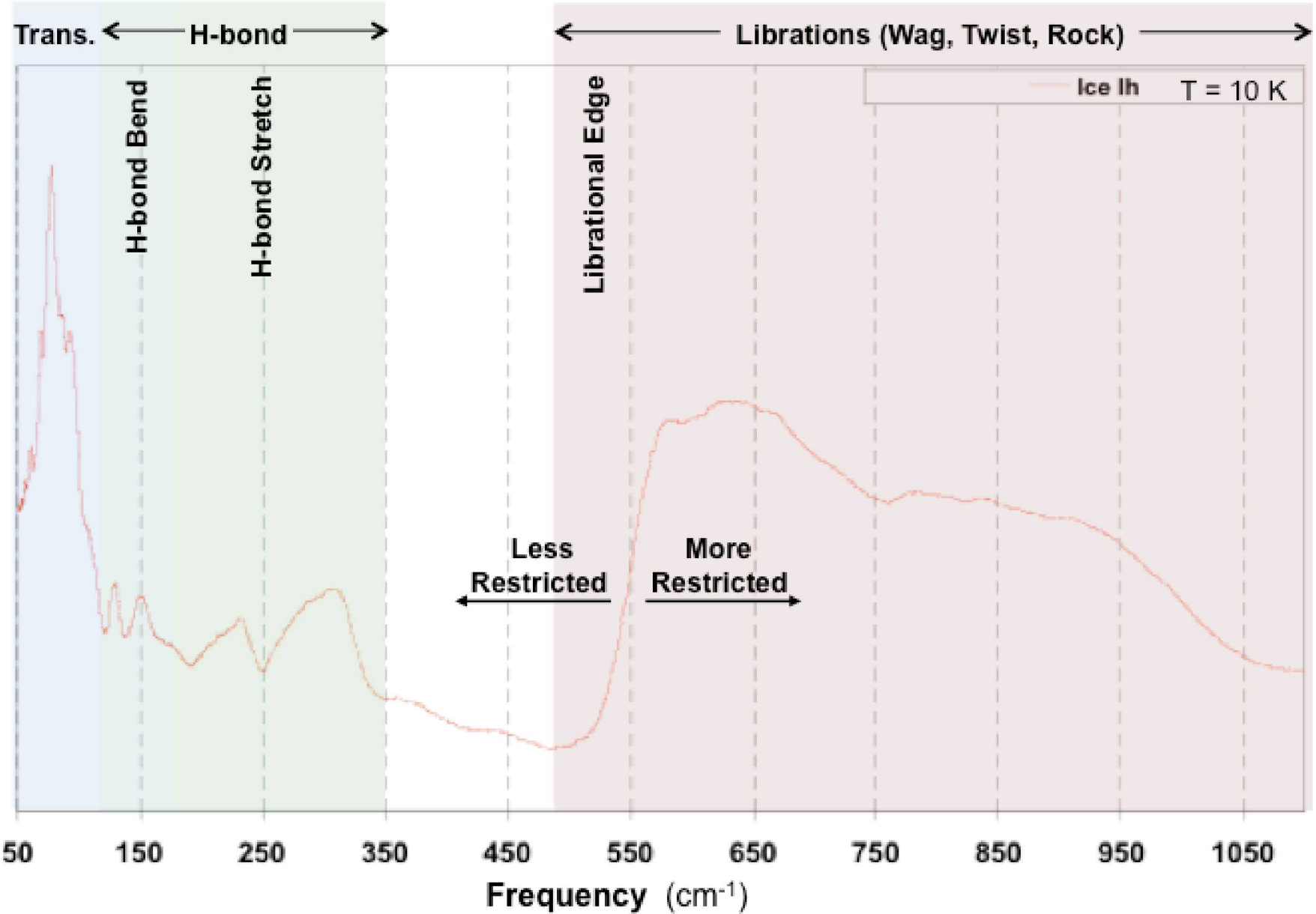

Behavior of Occluded Water in Zeolites, with Varying Si/Al

Clinoptilolite and Heulandite:

$[Mg,Ca,Na,K]_{4\text{-}6}[Al_6(Al,Si)_4Si_{26}O_{72}]\bullet 24H_2O$

- Most commonly occurring natural zeolite
- Abundant supply for many industrial applications
- Ion exchange capacities of ~2.5 meq/g
- Variable water content, cation, and Si/Al ratio

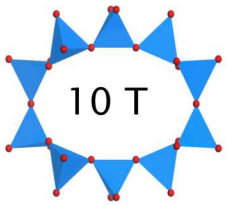

7.2 x 4.4 Å
orthonormal to *z*-axis

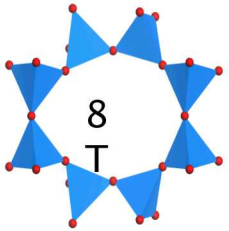

5.5 x 4.0 Å
orthonormal to *x*-axis

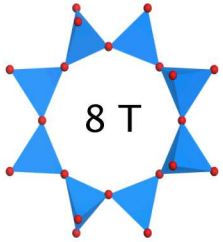

4.7 x 4.1 Å
diagonal to 10 T channels

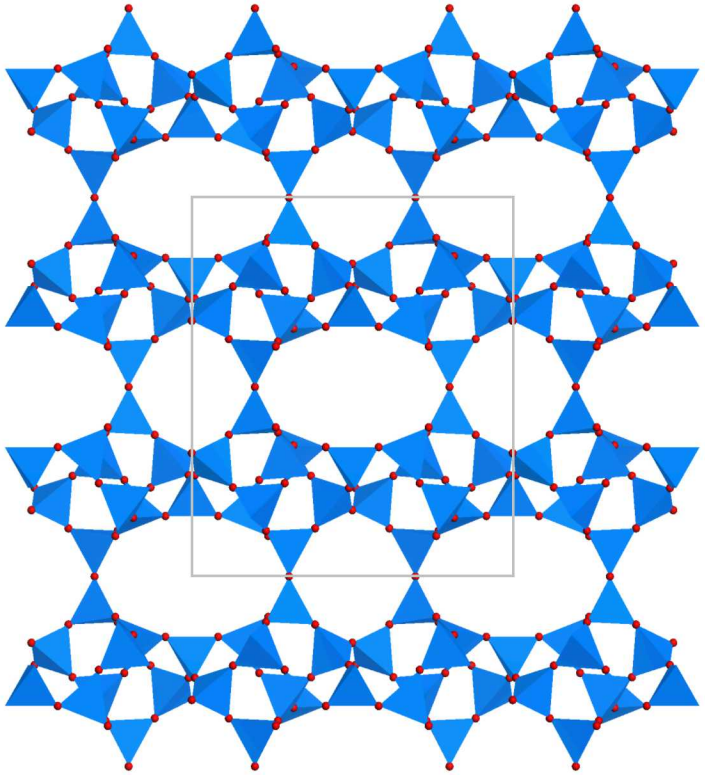

PCCP, **2008**, *10*, 800;
J. Phys. Chem. C., **2008,** *112,* 13629

Large-scale Molecular Dynamics (MD) Using LAMMPS

Calculated hydration enthalpies, radial distribution functions and ion coordination environments - used to describe the energetic and structural components of ions and occluded water

Flexible Framework Flexible SPC water	Clinoptilolite (Si/Al = 5.0)	Heulandite (Si/Al = 3.5)
Alkali	Li^{+}, Na^{+}, K^{+}, Rb^{+}, Cs^{+}	Li^{+}, Na^{+}, K^{+}, Rb^{+}, Cs^{+}
Alkaline Earth	Mg^{+2}, Ca^{+2}, Sr^{+2}, Ba^{+2}	Mg^{+2}, Ca^{+2}, Sr^{+2}, Ba^{+2}
Water Content	0→32/u.c.	0→32/u.c.
1 u.c. 114-210 atoms	Supercell (2x2x5u.c.) 2300-4200 atoms	500 ps Equilibration 250 ps Production Energetic Structural Spectroscopic
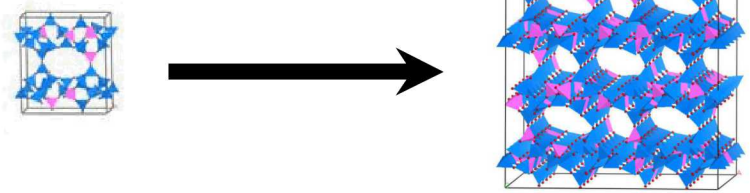		

Structure and Hydration - Zeolite Lowers the Ion Hydration Energy

Ion-O_w Distances (Å)

Δ_{max} ~ 10 %

		Li^+	Na^+	K^+	Rb^+	Cs^+	Mg^{2+}	Ca^{2+}	Sr^{2+}	Ba^{2+}
Soln	Pure H_2O (exp)	2.10	2.41	2.80	2.92	3.14	2.07	2.33	2.60	2.90
	Pure H_2O (calc)	1.88	2.33	2.83	2.98	3.18	2.23	2.60	2.98	2.93
Zeo	CLI-H_2O (calc)	1.88	2.29	2.82	2.94	3.06	1.99	2.43	2.68	2.75
	HEU-H_2O (calc)	1.89	2.28	2.81	2.92	3.02	1.98	2.91	3.15	3.19

Ion Hydration Enthalpies (kcal/mol)

		Li^+	Na^+	K^+	Rb^+	Cs^+	Mg^{2+}	Ca^{2+}	Sr^{2+}	Ba^{2+}
Soln	Ion (exp)	-124	-97	-77	-71	-66	-459	-377	-345	-312
	Ion (calc)	-127	-101	-69	-66	-62	-433	-358	-311	-314
Zeo	CLI (calc)	-160	-142	-128	-124	-122	-98.8	-184	-176	-168
	HEU (calc)	-181	-152	-130	-126	-111.9	-95.0	-155	-153	-151

CLI and HEU calculated on a per H_2O Basis

$\Delta H^{ion}_{hyd} = [\langle U_{wat + ion}\rangle - \langle U_{wat}\rangle] / nH_2O$; $\Delta H^{ion+frame}_{hyd} = [\langle U_{wat + ion + frame}\rangle - \langle U_{ion + frame}\rangle] / nH_2O$

Ion Coordination Environment

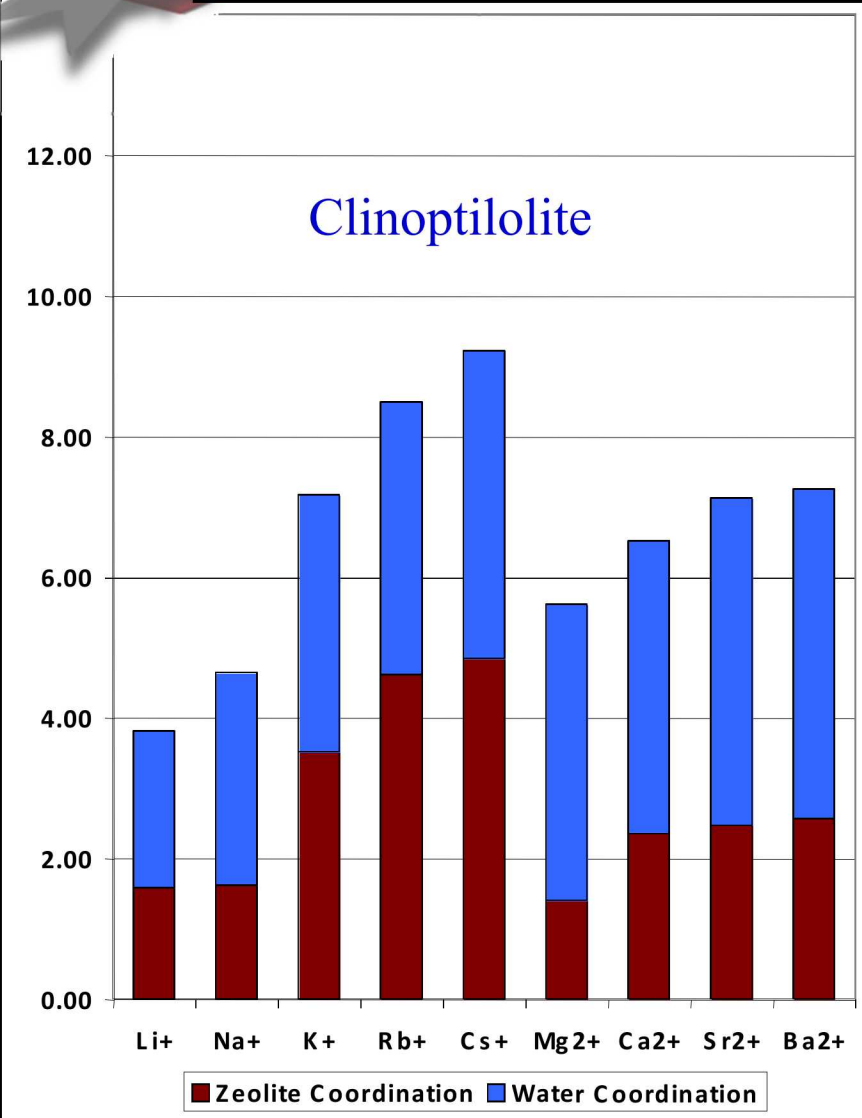

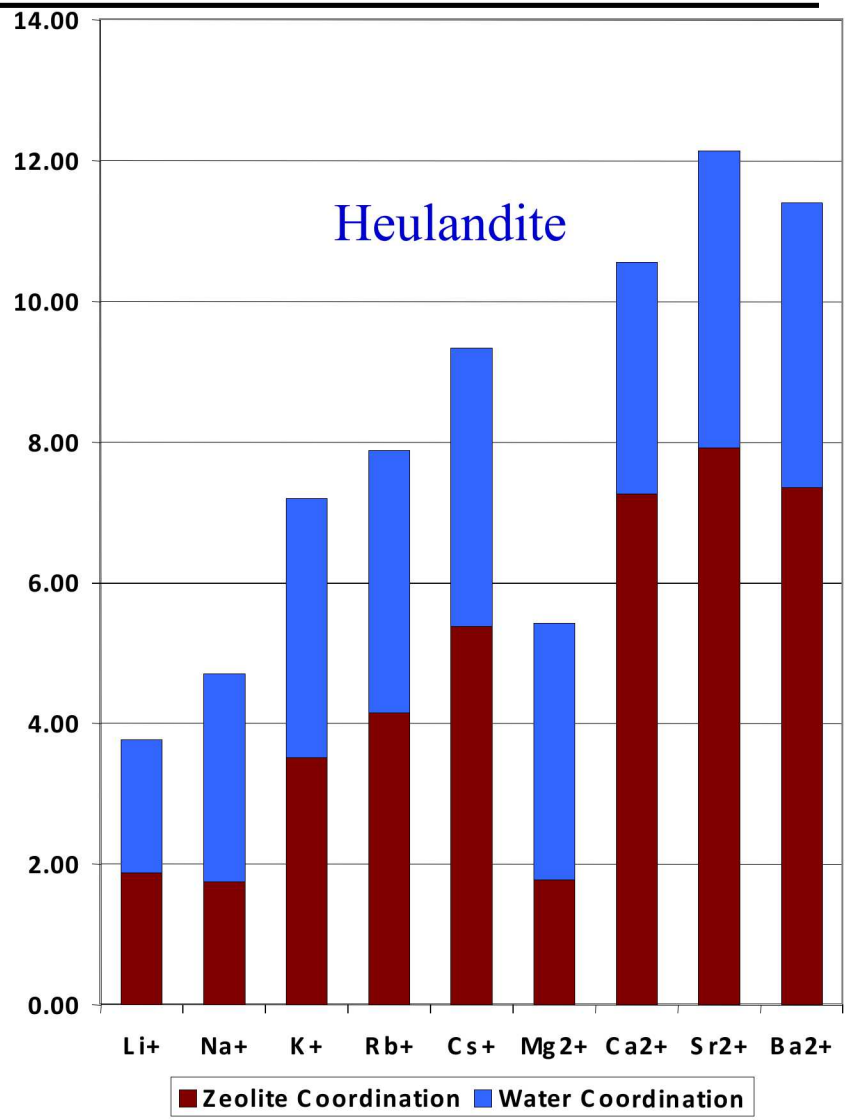

Less Negatively Charged Framework

More Negatively Charged Framework

Effect of Zeolite Pore Confinement & Framework Composition (Acidity)

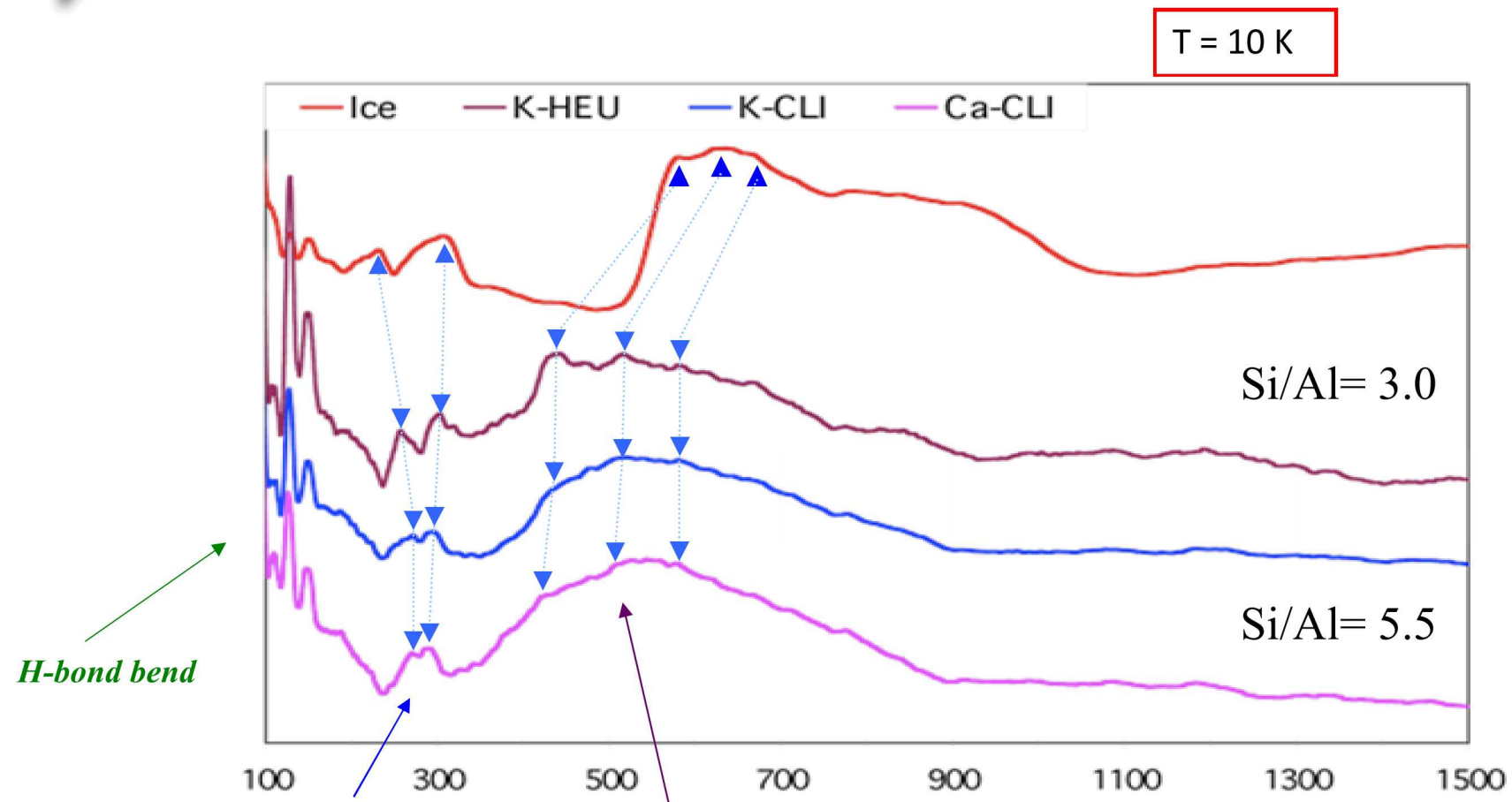

H-bond bend

H-bond stretch
Affected by framework acidity

Libration modes:
Less Restrictive : Decreased H-bonding vs. Ice
Broadening: multiple water modes (different water configurations)
(24 Occluded H_2O molecules/unit cell

Trends in the Inelastic Neutron Scattering (INS) Data Match the predicted trends

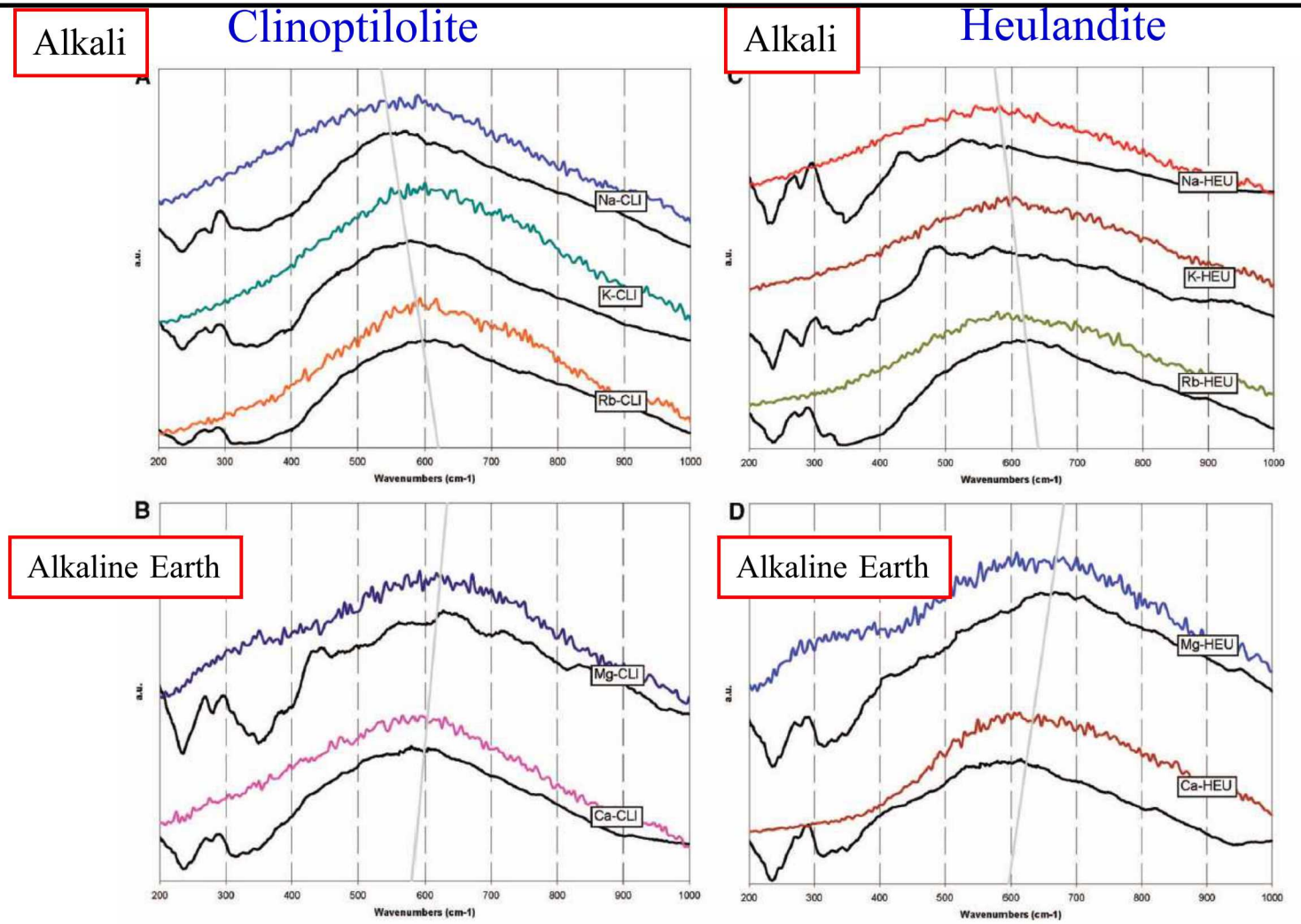

Librational Shift versus Ion Charge Density

Exp: Monovalent cations, H_2O trends to framework

Exp: Divalent cations, H_2O trends to cation

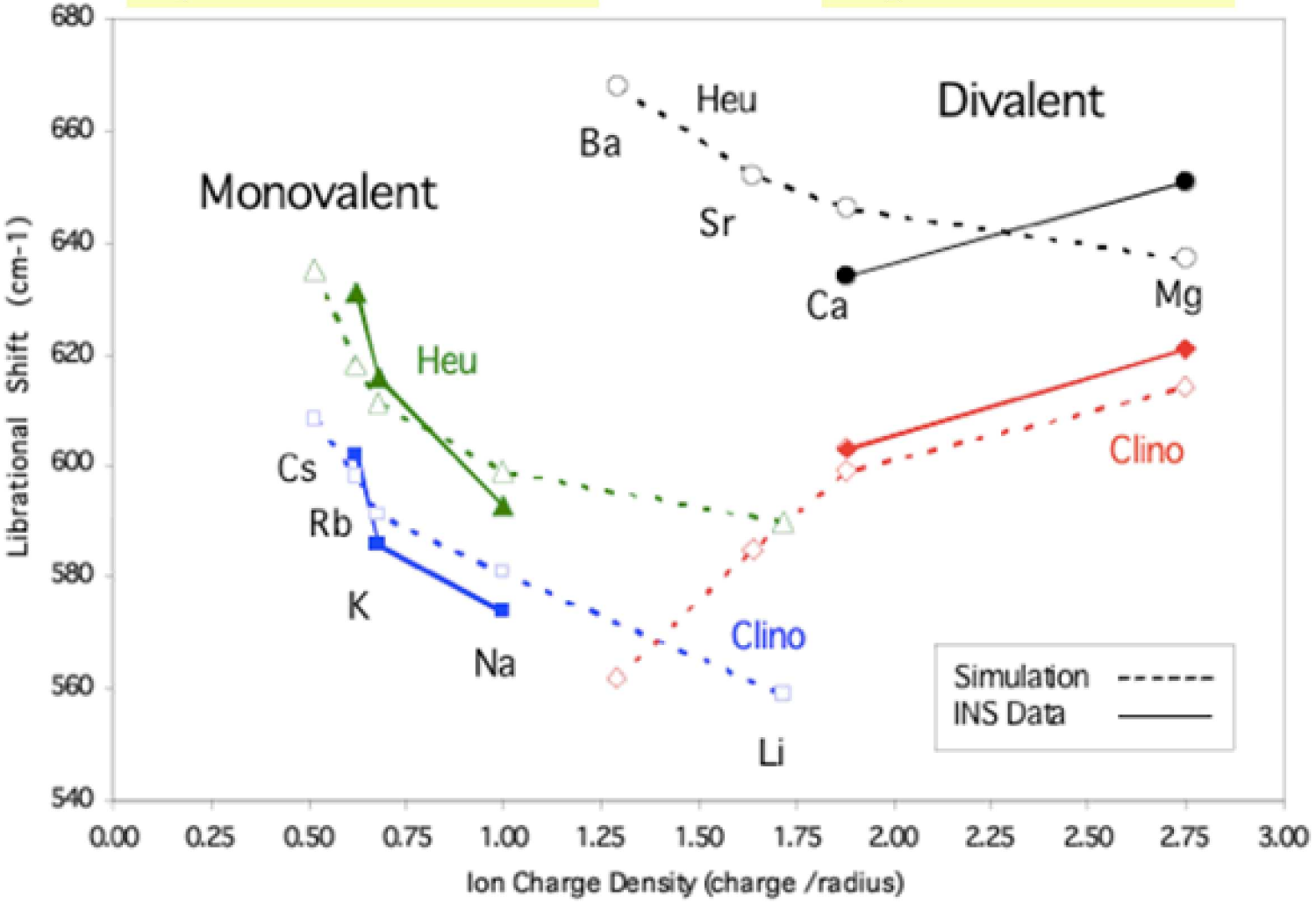

R&D Area 2: Nanoparticle Formation

I. Chemical loading, *reduction and activity*

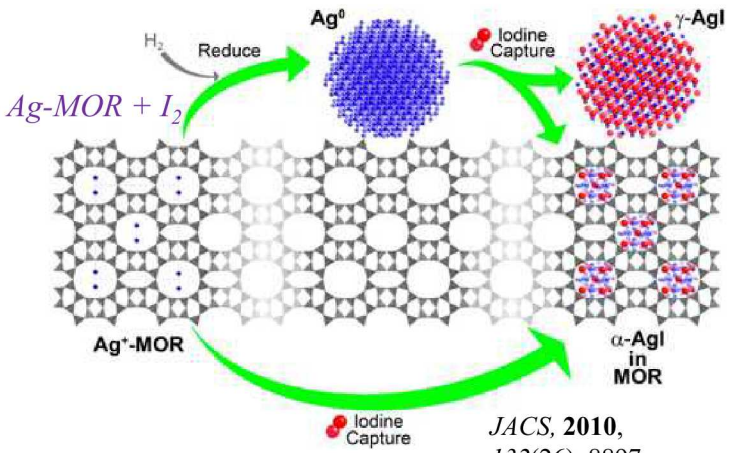

JACS, **2010**, *132*(26), 8897

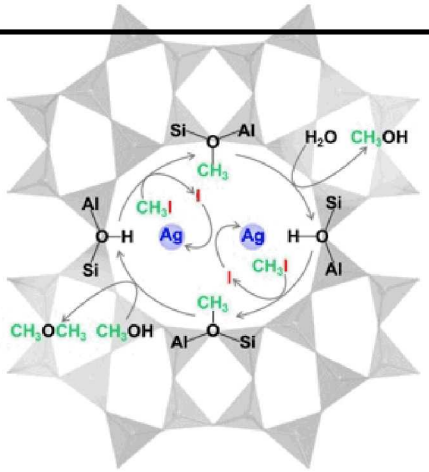

Ag-MOR + CH_3-I

MMM, **2014**, *200*, 297

PDF study of Ag NP formation and migration

JPC Letters, **2011**, 2, 2742

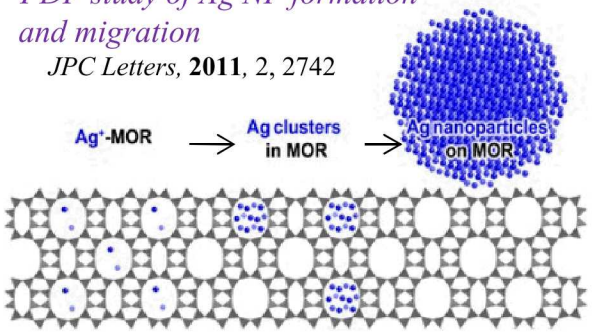

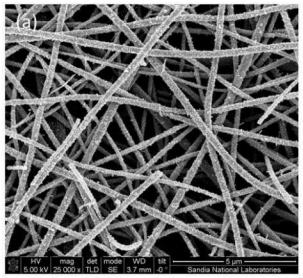

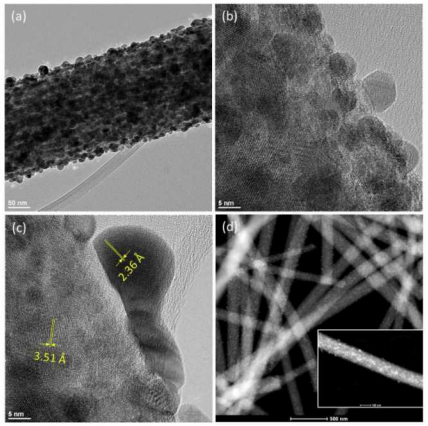

II. Electrospun

nonwoven TiO_2 crystalline mesoscale fibers & Ag. Ag^+ spun, NPs reduced both in nanopores and on nanofibers. Also AgI, and ZIF-8 NPs.

Patent pending, 2019
SAND2012-8025

III. Radiolysis *for the generation of e^-_{aq}, Chem reduction of metal salts NPs, free standing or supported*

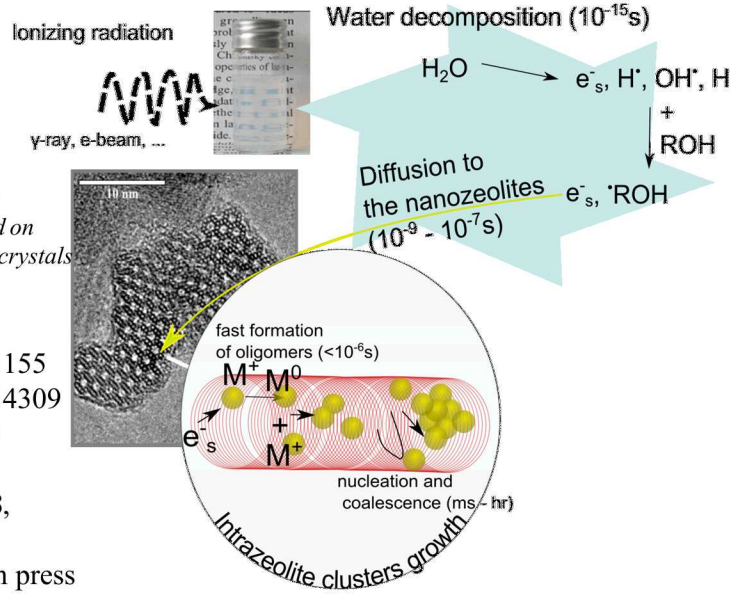

Pulse Radiolysis: Ag NPs supported on BEA zeolite nanocrystals

J. Phys. Chem.C, **2009**,*113*, 1155
J. Phys. Chem.C, **2010**,*114*, 14309
Chem. Mater., **2011**,23, 5185
J. Nuc. Mat, **2013**, *442*, 162
Invited Review: *JPCC*, **2018**, *122*(24), 12573
Nanoscale Advances, **2019**, in press

Ag-MOR zeolite, Nanoparticles for gas capture

- While I^{129} is only found in small concentrations in nuclear effluent, the effective capture and storage of iodine is critically important to public safety due to its involvement in human metabolic processes and its long half-life ($\sim 10^7$ years).

- Silver Mordenite (MOR) is a standard iodine-getter, although the iodine binding mechanism remains poorly defined. Presumably an iodide forms within the zeolite's pores

- Understanding **Structure-Property Relationship between Nanoscale and Bulk effects**
  - To optimize capture
  - Impacts processing for long term storage
  - To predict long term stability

MOR, Mordenite

$X_2Al_2Si_{10}O_{24}\bullet 7(H_2O)$

12 MR, 7.0 x 6.5Å

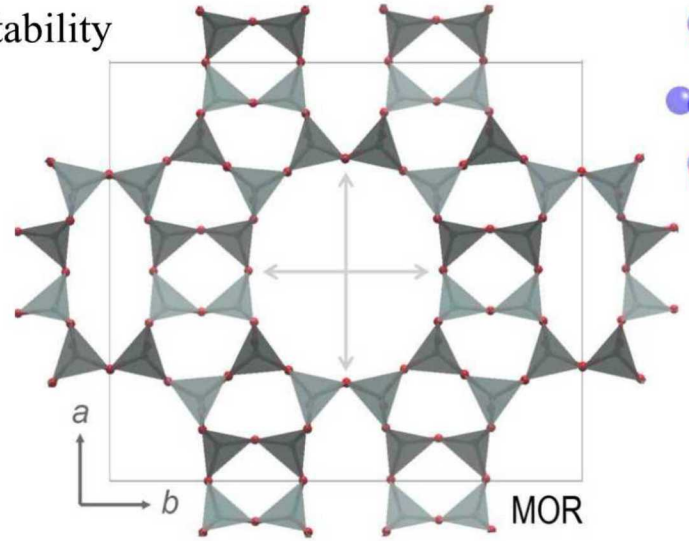

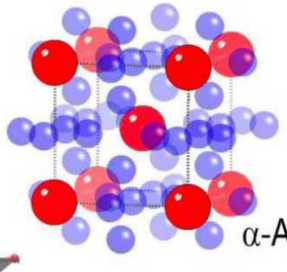

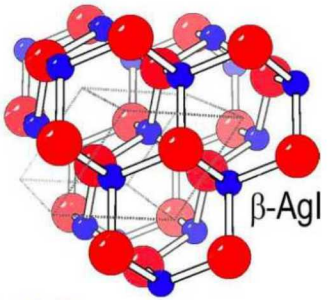

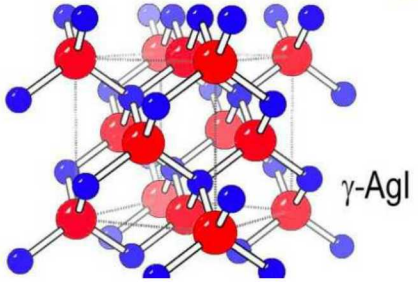

Fundamental Studies of AgI-Zeolites: Ag-Mordenite (MOR) industry standard for I_2 capture

Mordenite Topology and AgI Polymorphs

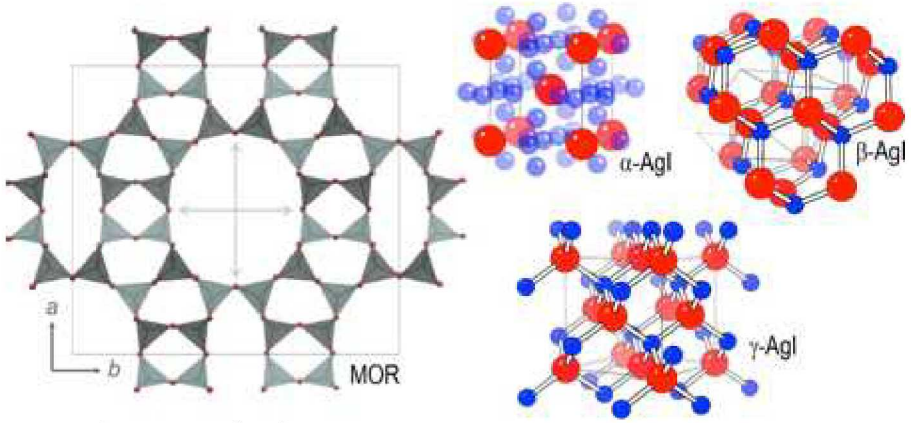

MOR, Mordenite

$X_2Al_2Si_{10}O_{24}\bullet 7(H_2O)$

12 MR, 7.0 x 6.5Å

Idealized MOR framework: *Used for Decades*

- 1D channels (12-rings, 6.5 x 7.6 Å) which contain exchangeable cations and water molecules (omitted).
- α, β, γ-AgI polymorphs (iodine-red; silver-blue)

MOR Samples from UOP: LZM5
I_2 gas exposure, saturated environment, 95°C
Ag reduction, 3% H_2 stream, 150°C

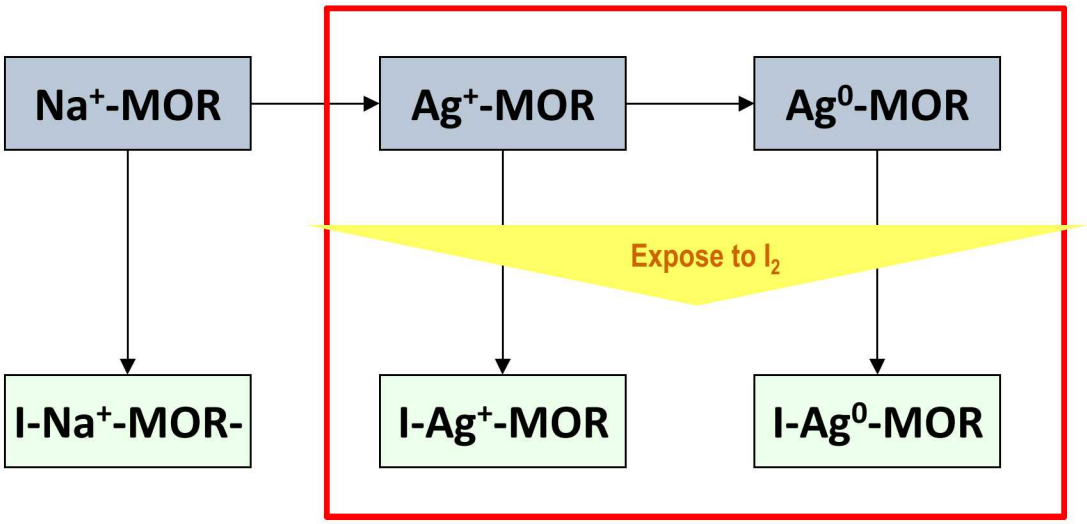

To study the capture of Iodine by either ion exchange or reduced Ag-MOR, samples were analyzed at ANL/APS by Pair Distribution Function (PDF) analysis

PDF measurements: APS/ANL Collaboration

Does it matter which synchrotron?

Yes. Only higher energy storage rings produce significant fluxes of high energy X-rays

High energy X-rays are a unique strength of the *Advanced Photon Source* (in the western hemisphere)

- 3 dedicated high energy beam lines
- 1 dedicated PDF beamline

APS 11-ID-B: Dedicated PDF facility
- 58 or 90KeV high energy X-rays
- typical wavelengths = 0.1 - 0.2Å

For our experiments:

$Q > 20Å^{-1}$; CuK_α to $2\Theta = 180$ results in $Q_{max} = 8Å$

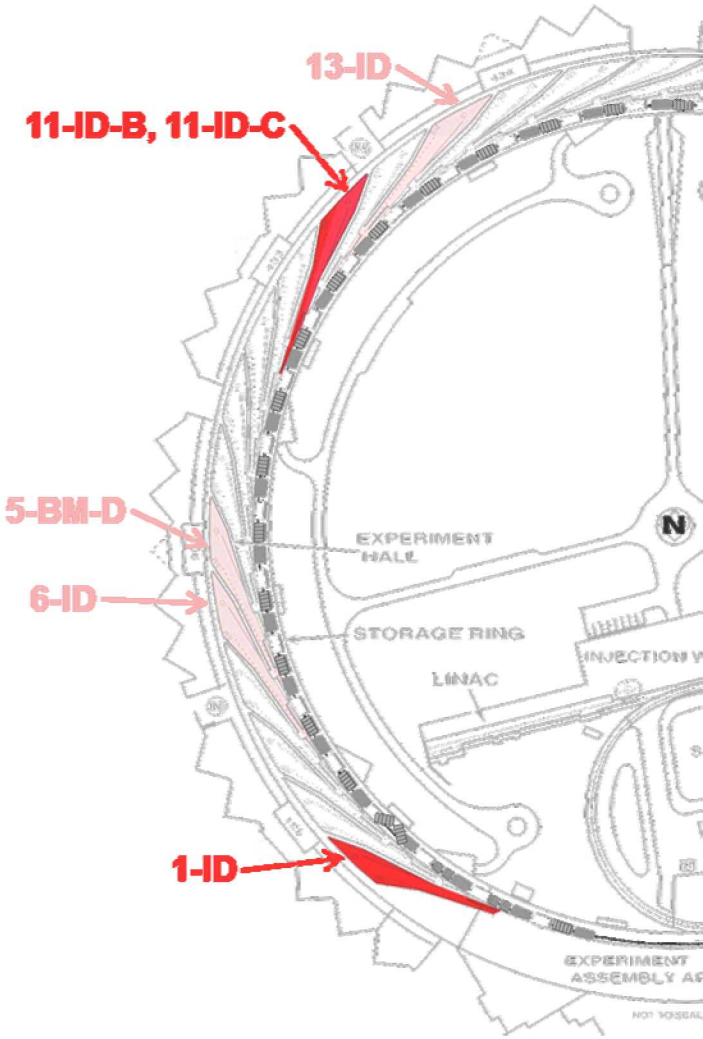

Differential-PDFs: Fundamental Study of Zeolite Framework and Occluded AgI NPs

Synchrotron Pair Distribution Function Analysis (d-PDF) allows study of the AgI, minus the MOR zeolite framework (collaboration SNL & ANL/APS)

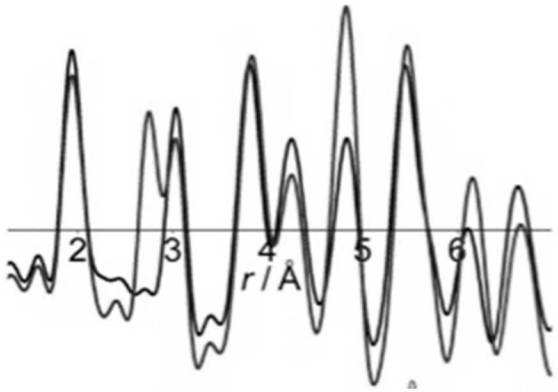

$G(r)_{Ag\text{-}I\text{-}MOR} - G(r)_{Ag\text{-}MOR}$

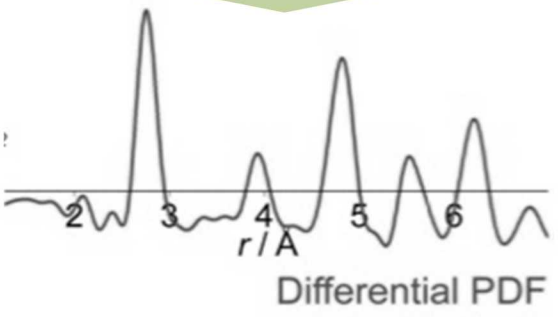

In-zeolite pore capture

	Form	*r*-range (Å)	R_{fit}	Phase Composition[§]			
				Ag^0	α-AgI	β-AgI	γ-AgI
Ag^+-I	on MOR	2-10	27.5%	–	1	–	–
Ag^0-I	on MOR	2-30	18.0%	–	0.6	–	0.4
AgI (Aldrich)	bulk	2-30	13.6%	–	–	0.53	0.47
AgI (Ag^0+I_2)	bulk	2-30	7.97%	0.5	–	–	0.5
Ag^0	on MOR	2-30	9.15%	1	–	–	–

[§] Ag^0 (*Fm*-3*m*, $a = 4.08$ Å); α-AgI (*Im*-3*m*, $a = 5.0$ Å, $r < 7$ Å); β-AgI ($P6_3mc$, $a = 4.6$ Å, $c = 7.8$ Å, wurtzite structure); γ-AgI (*F*-43*m*, $a = 6.5$ Å, zinc blende structure).

Mechanism Determined: State of the Ag determines I capture

Ag°-MOR + I_2 yields a mixture of γ-AgI bulk surface nanoparticles and sub-nanometer α-AgI.
Ag^+-MOR + I_2 produces exclusively sub-nanometer α-AgI ("**perfect fit**", confined in pores)

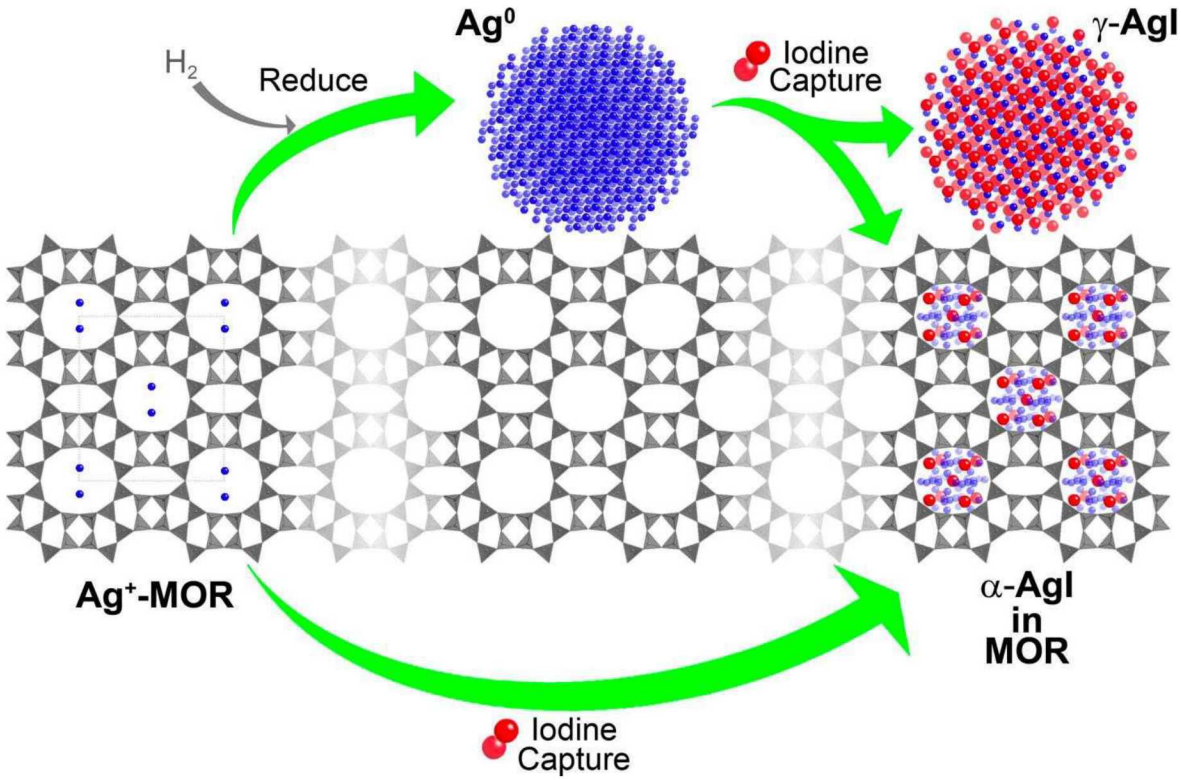

JACS, **2010**, *132* (26), 8897

*Issue associated with Zeolites do include the **need for Ag** and the difficulty of working with zeolites that **selectively adsorb I_2 and Org-I,** but **not ^3H_2O, and Xe***

In-situ Monitoring of Ag Nanoparticle Formation in Zeolite MOR (from Ag^+-MOR)

Study Conversion and Migration of Ag^+ to Ag° in MOR

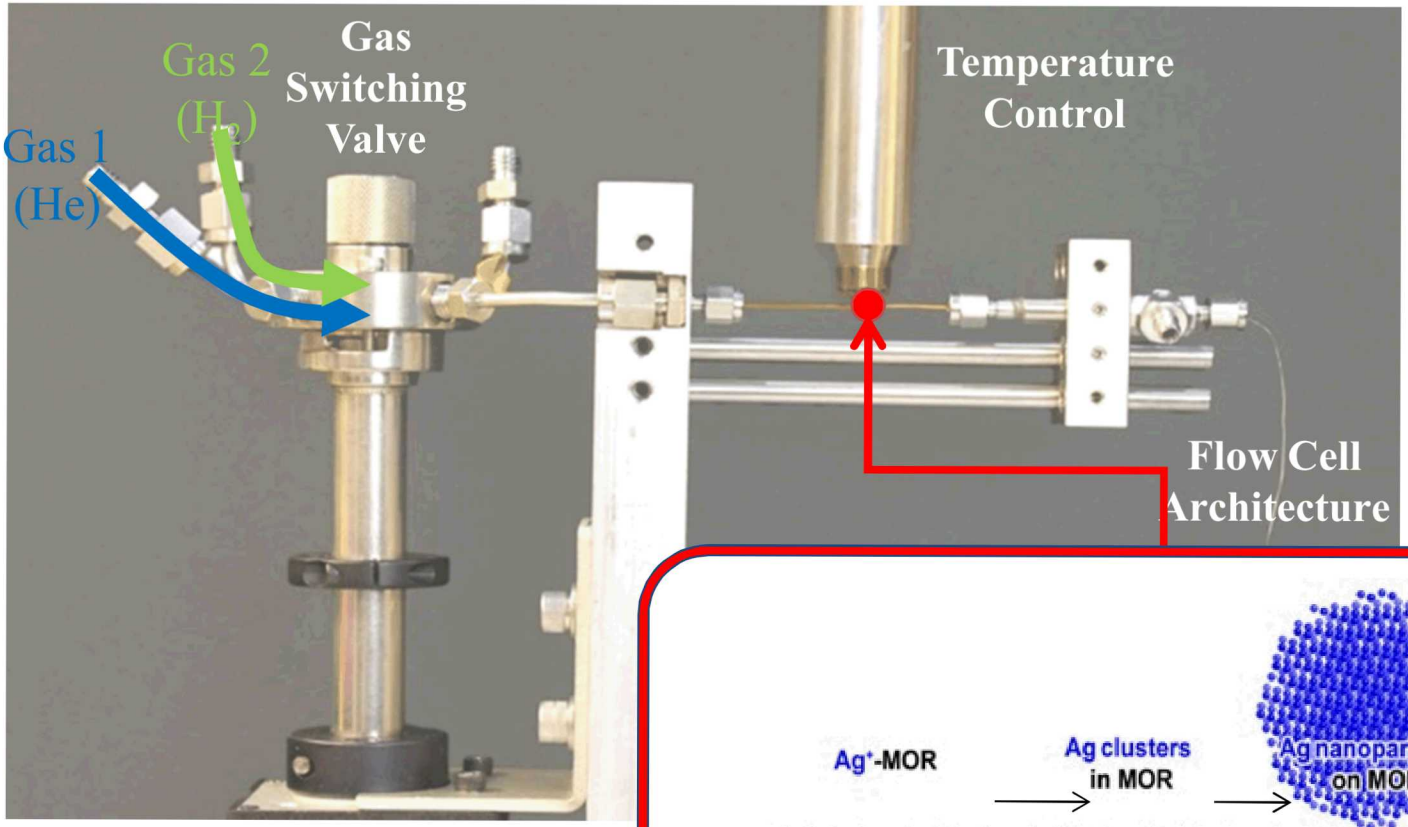

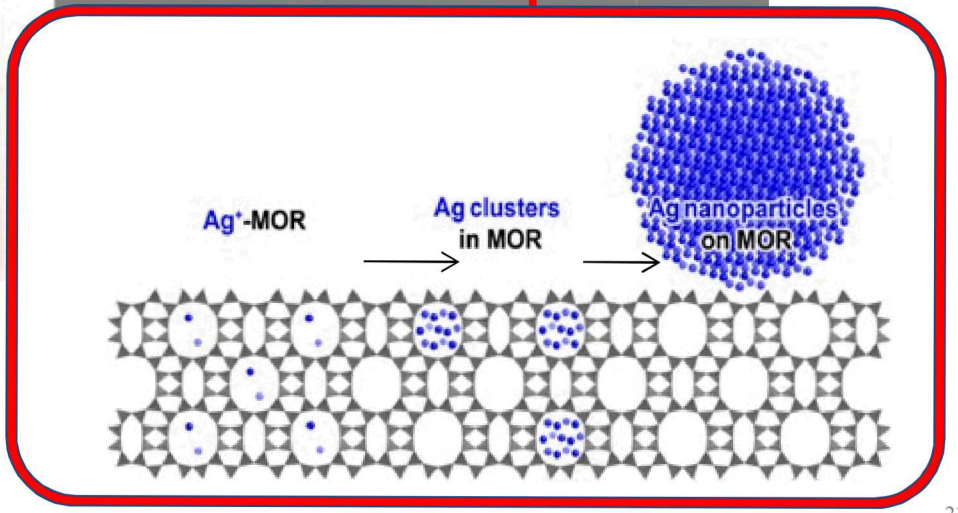

In situ I_2 sorption on Ag-MOR using PDF setup at 11-ID-B beamline at APS/ANL

In situ studies of Ag catalyst formation

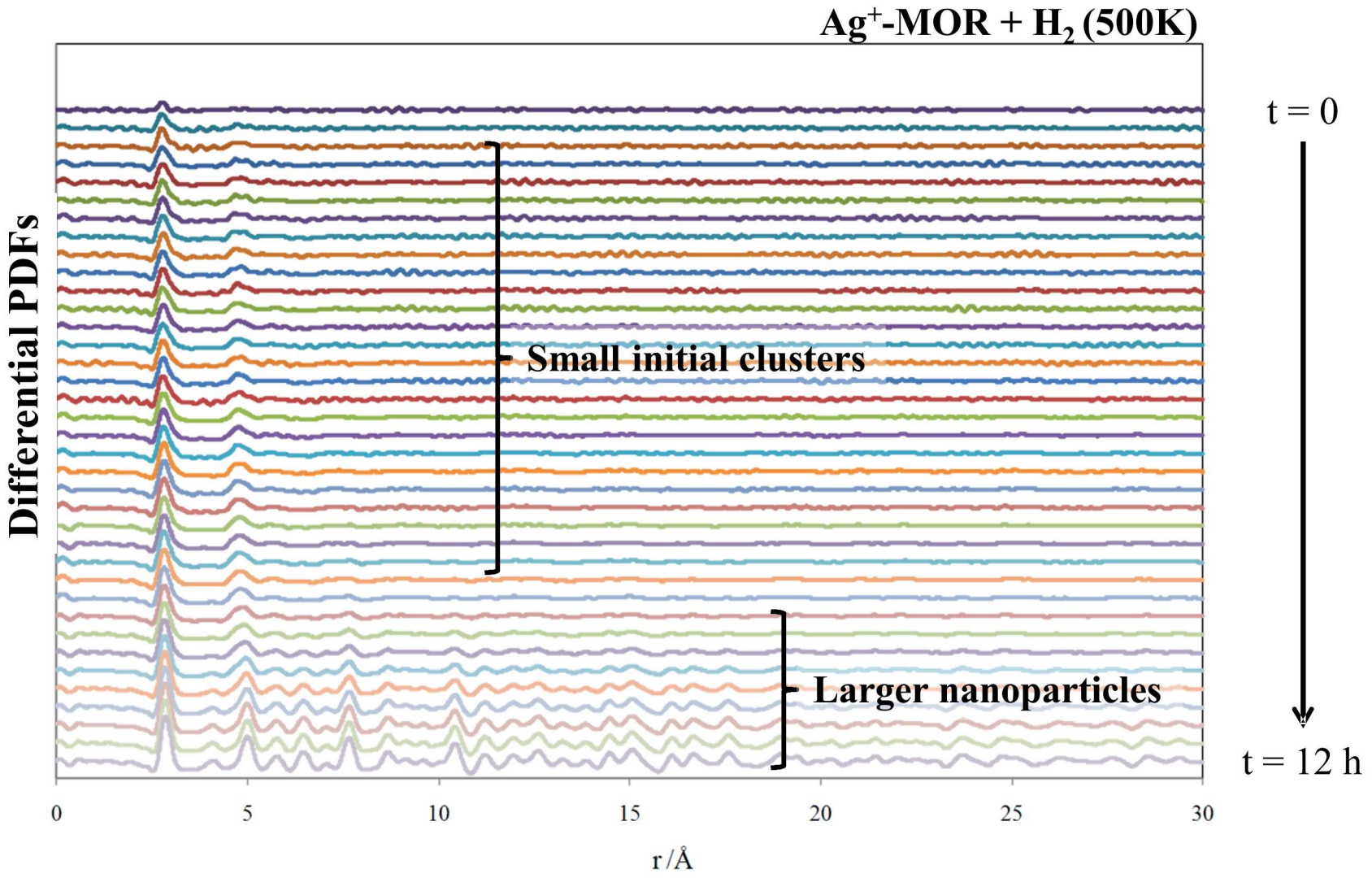

Quantitative insights from in-situ pdf data collection: Gaussian peak fitting

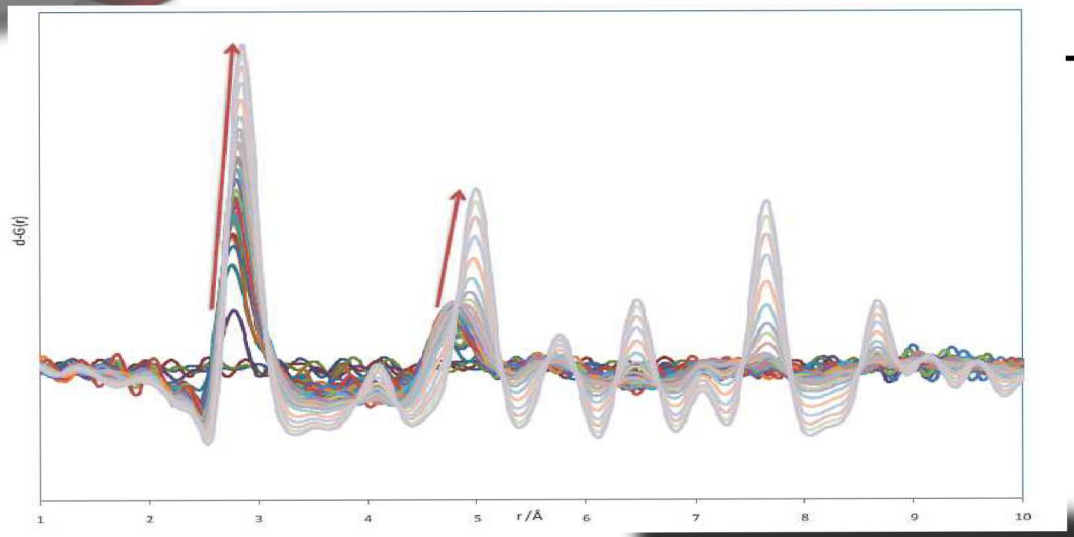

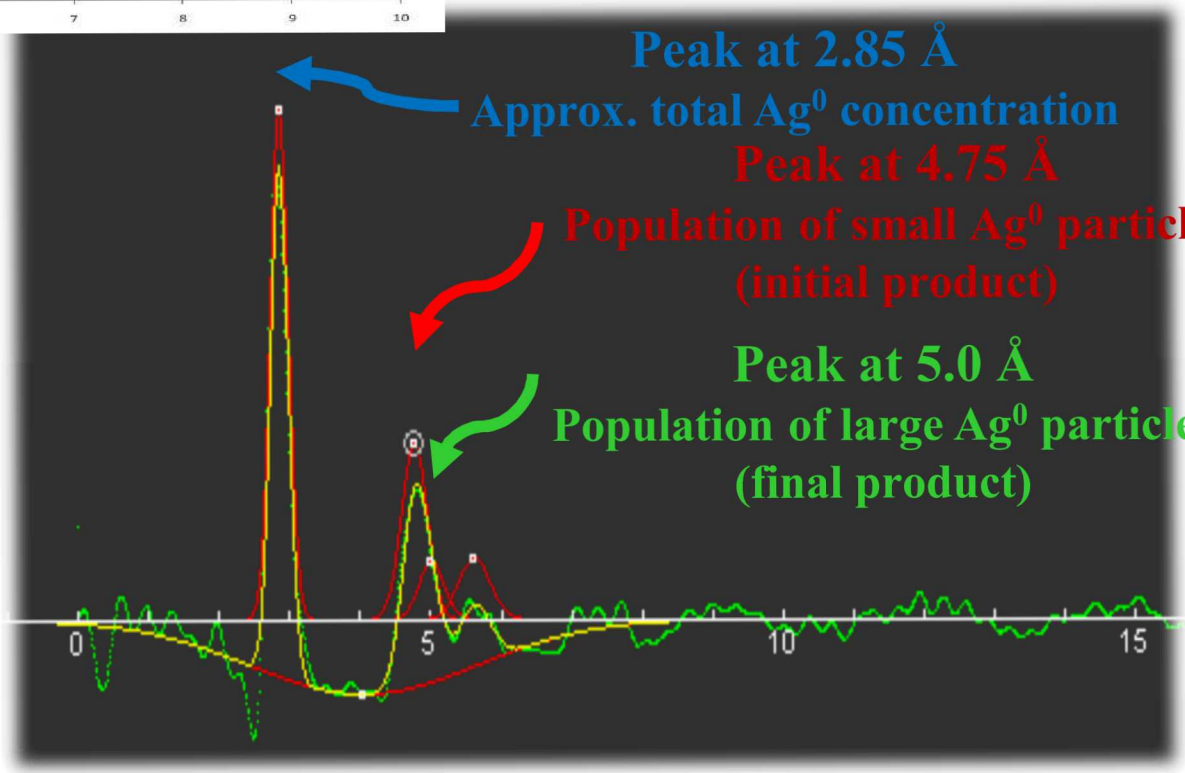

Reaction profile

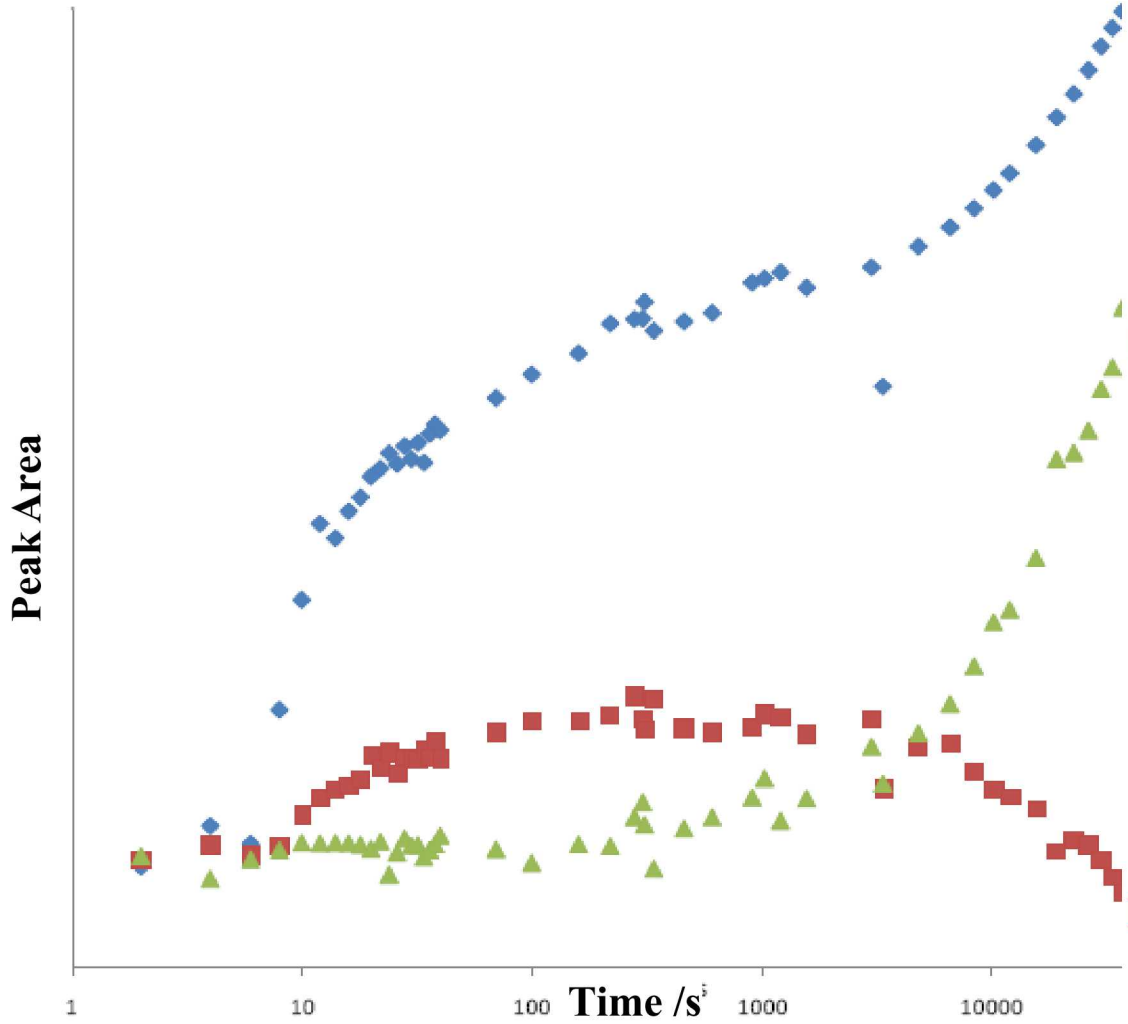

Peak at 2.85 Angstrom
Approx. total Ag^0 concentration

Peak at 5.0 Angstrom
Population of large Ag^0 particles
(final product)

Peak at 4.75 Angstrom
Population of small Ag^0 particles
(initial product)

Multi-step Mechanism for Silver Particle Growth and Migration on a Porous Zeolite

i) Ag^+ reduction in 12MR and 8MR "Red star"
ii) Ag° migration from 8MR to 12MR
iii) Ag° form clusters within 12MR channels
iv) Clusters migrate to zeolite surface
v) Clusters aggregate as nanoparticles

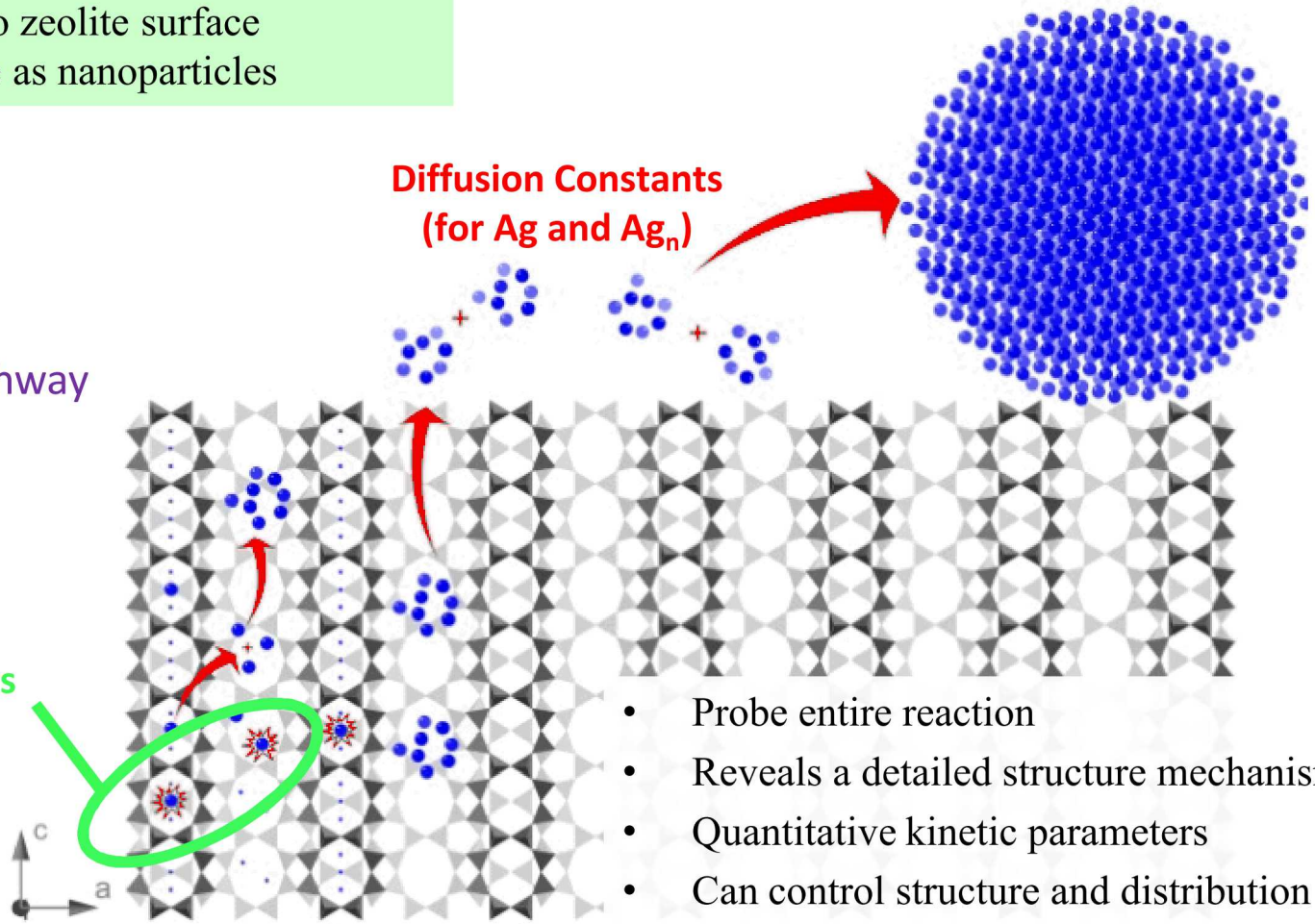

- Probe entire reaction
- Reveals a detailed structure mechanism
- Quantitative kinetic parameters
- Can control structure and distribution

J Phys Chem Letters, **2011**, *2*, 2742

Broader Question: Does Dehydration play a role in Ag-Zeolite nanoparticle formation?

X-ray see heavy species well (Ag) but not the surface molecules (H_2O, OH, etc) that control the surface chemistries of the zeolites:

PDF + DRIFTS provides both complimentary methods

Ag nanoparticle formation induced by: Reduction or Dehydration?

Experiment:

Variable temperature PDF + DRIFTS studies in reducing & inert atmosphere

- Three zeolites of differing framework and pores structure, and Si/Al ratio
- Heat 25 - 330°C while collecting data
- Monitor NP formation with transitions in water/hydroxides bonding & presence in zeolite
- Determine most important parameters & mechanisms

T. M. Nenoff, tmnenof@sandia.gov

Tuning the reaction environment in other zeolites

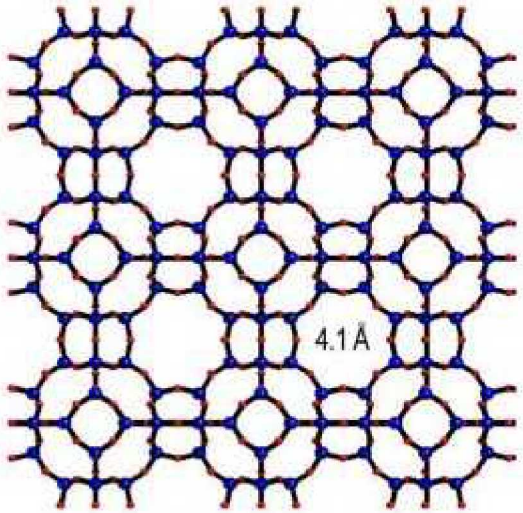

LTA (A)

Si/Al = 1

Most Ag^+ /surface -OH

Small pores only

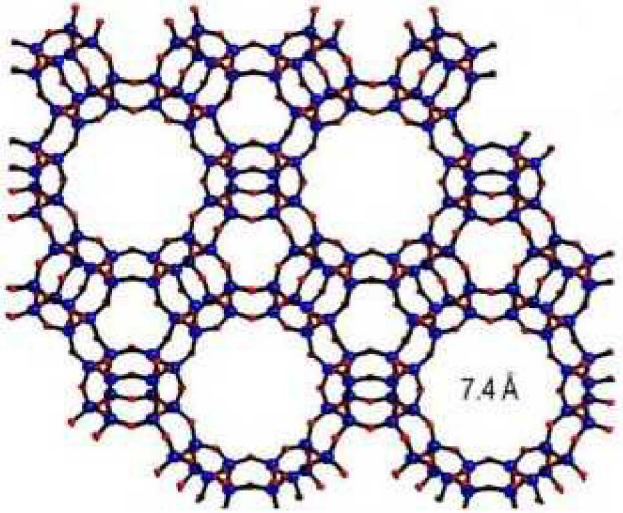

FAU (Y)

Si/Al = 2.4

Intermediate Ag^+ /surface -OH

Large pores

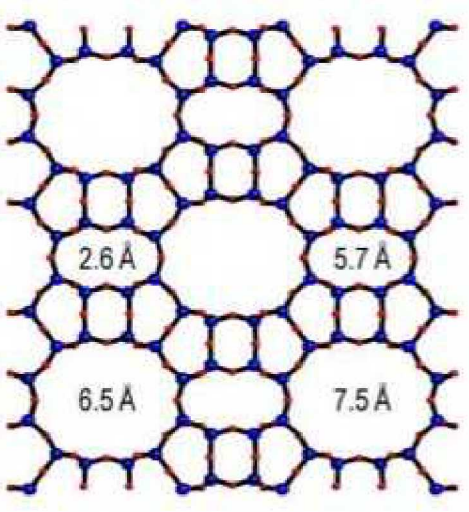

MOR

Si/Al = 5

Least Ag^+ /surface -OH

Large & small pores

Nanoparticle formation pathway varies widely

Different onset temperatures, stability window for Ag clusters, final NP size

Inert atmosphere: Small clusters persist over large temp range

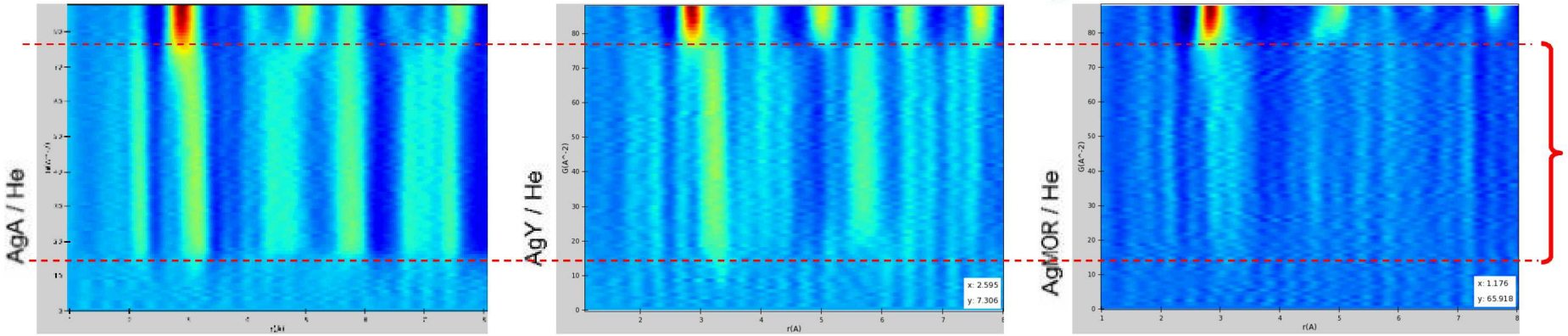

LTA (A) FAU (Y) MOR

Reducing atmosphere: Small clusters & larger nanoparticles form ~ in rapid succession

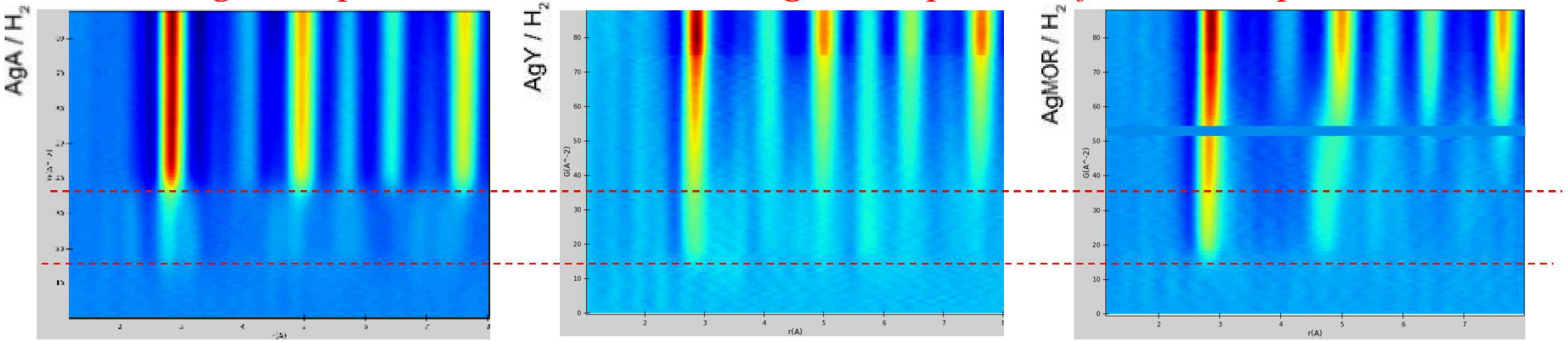

Filling in the missing pieces - PDF$^+$

Complementary insights from multimodal measurements

What role does dehydration play in the Ag nanoparticle formation?

- The PDF signal is dominated by high Z species
- Complementary, compatible infra-red spectroscopy is sensitive surface species (H_2O/OH)

DRIAD-X: Diffuse Reflectance Infrared Angular Dispersive X-ray Measurements

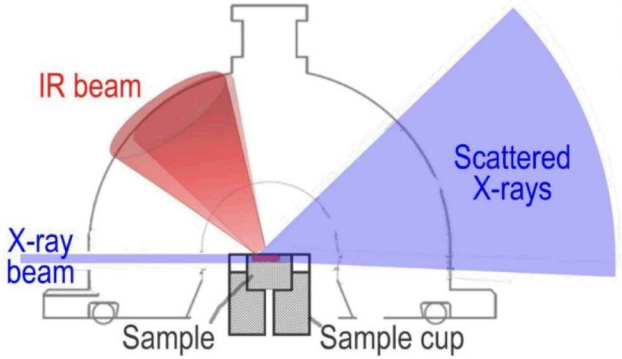

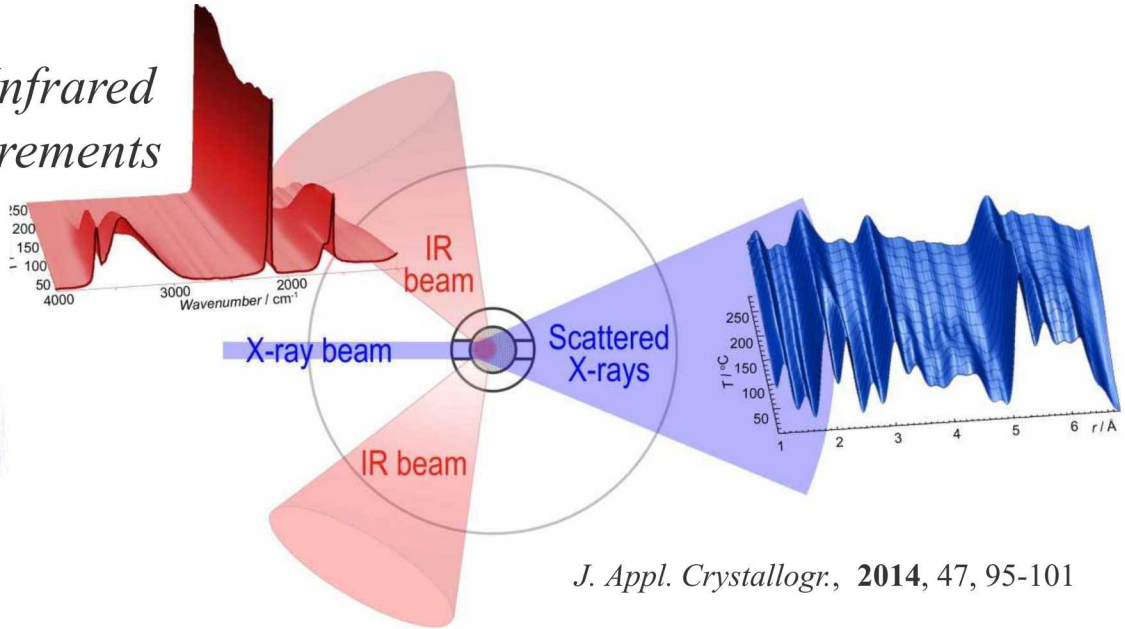

J. Appl. Crystallogr., **2014**, 47, 95-101

New approaches to quantify chemical reactivity

Operando PDF

- Captures entire reaction
- Provides detailed structure mechanism and quantitative kinetics

Multimodal measurements (PDF+IR)

- Provides enhanced chemical insight & sensitivity
- Because a singular sample is being probed simultaneously, data can be compared directly without offsets associated with different sample environments

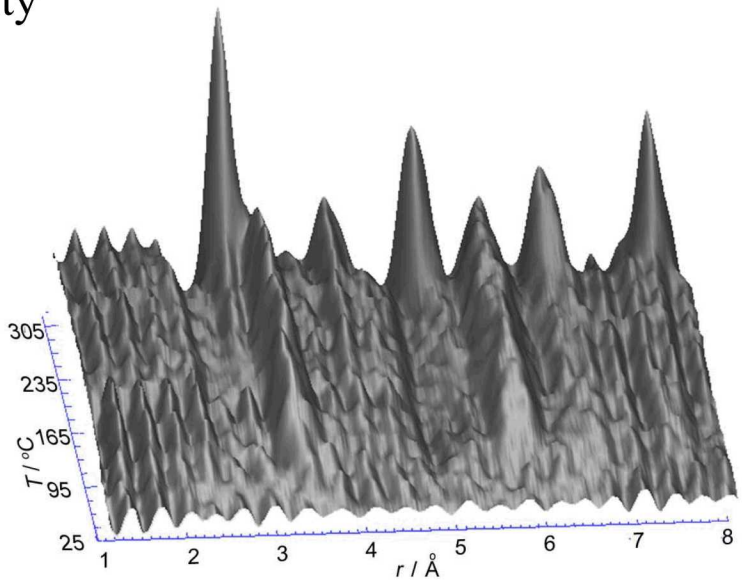

DRIFTS shows water and surface OH species

Loss of water and hydroxyl species evident in DRIFTS. Increasing baseline

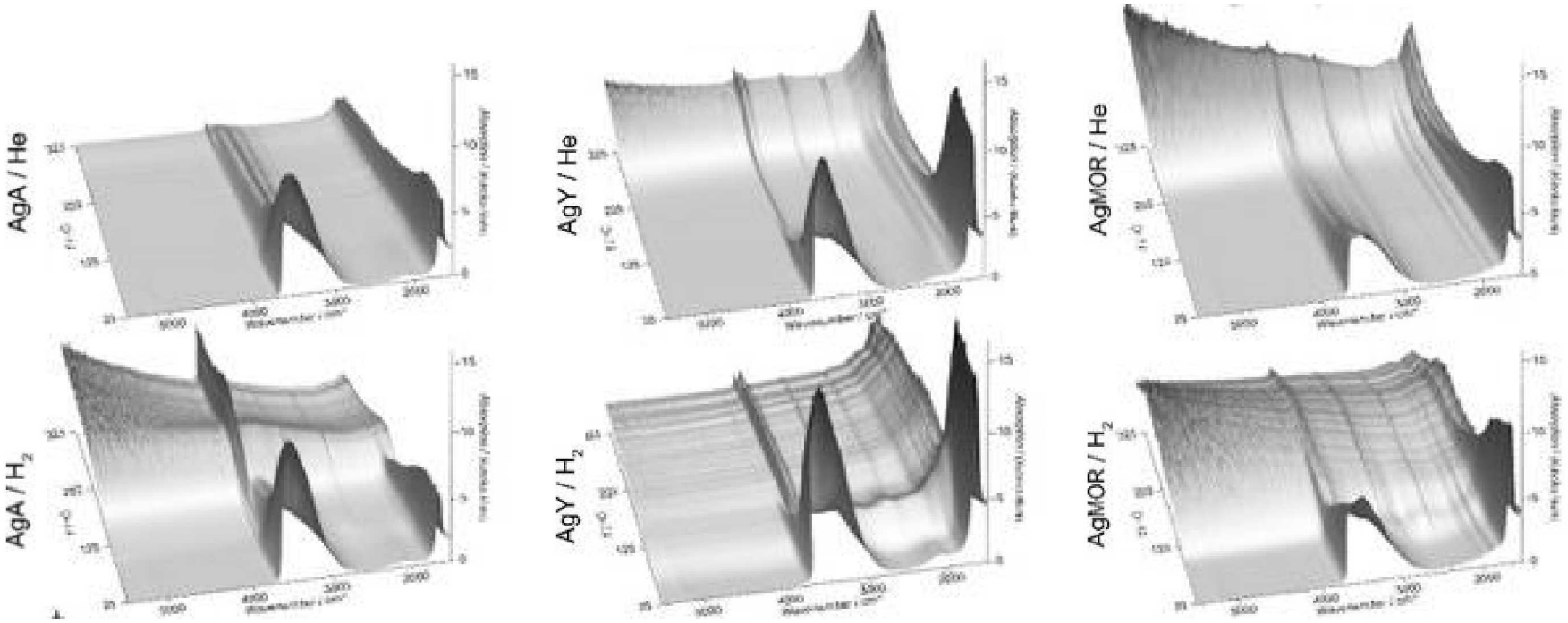

Nanoparticle Growth in Aluminosilicate Zeolites

(1) Chemistry of Framework

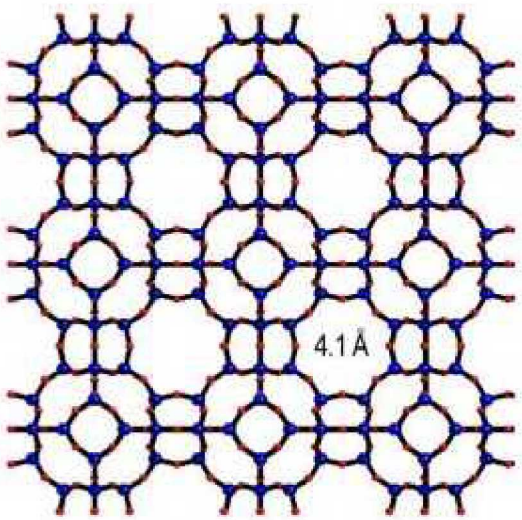

LTA (A)
Si/Al = 1

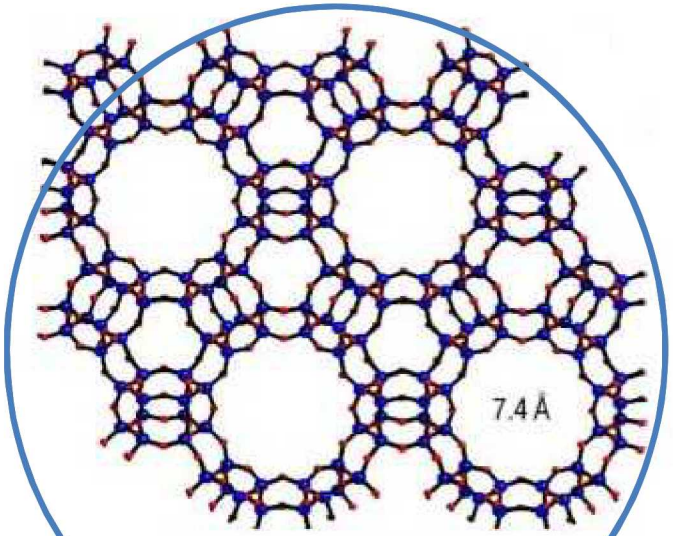

FAU (Y)
Si/Al = 2.4

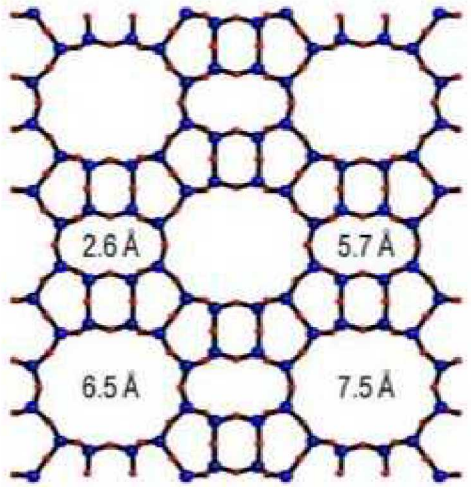

MOR
Si/Al = 5

(2) Chemistry of the reduction:

Autoreduction = Temperature with He

Reduction – H_2 reducing gas with temperature

Focus Today.
Data compiled for all 3 zeolites and 2 chemistries

Example of AgY Autoreduction

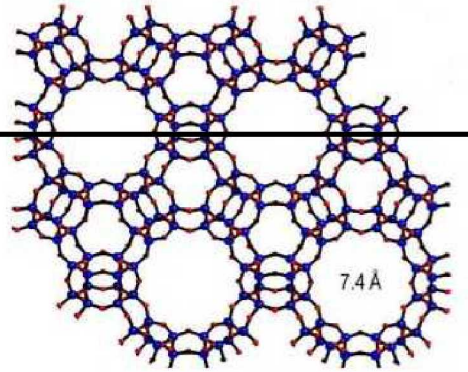

DRIFTS

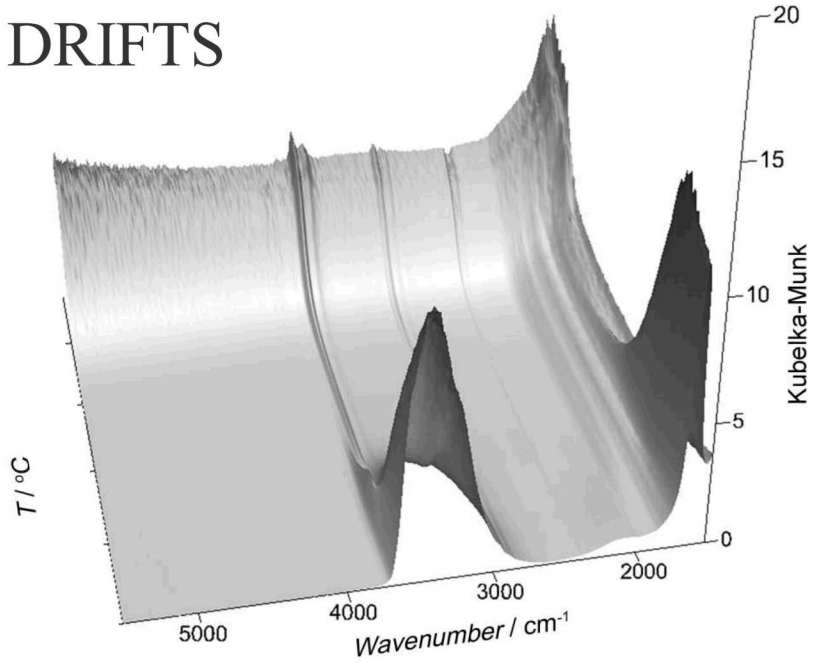

1) H_2O, OH stretches eliminated, then
2) Reflectivity decreases

PDF

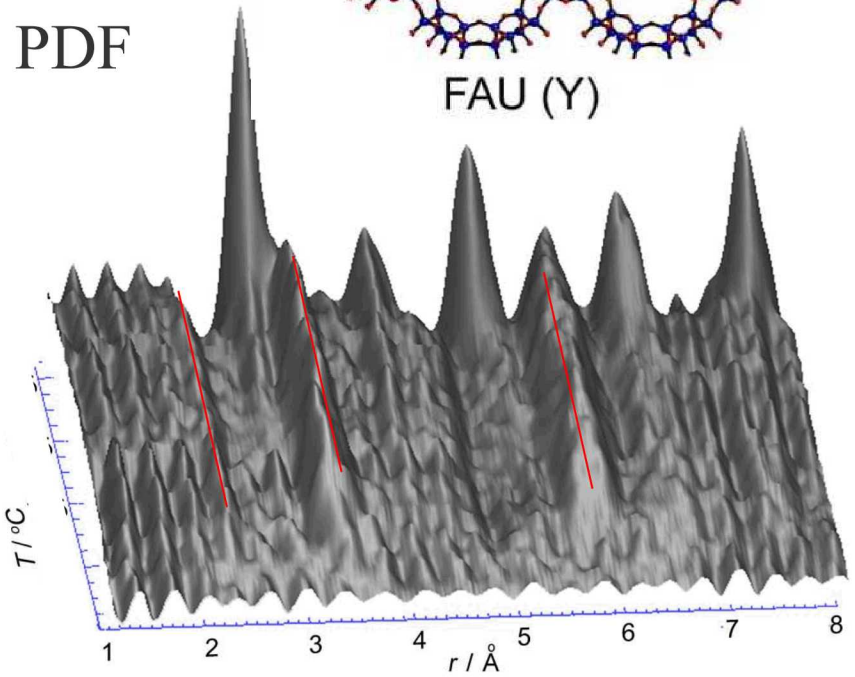

1) nm scale Ag_2O nanoparticle intermediate
2) Larger Ag nanoparticles

Correlating surface chemistry & NP formation

Surface chemistry governs cluster mobility and aggregation

DRIFTS

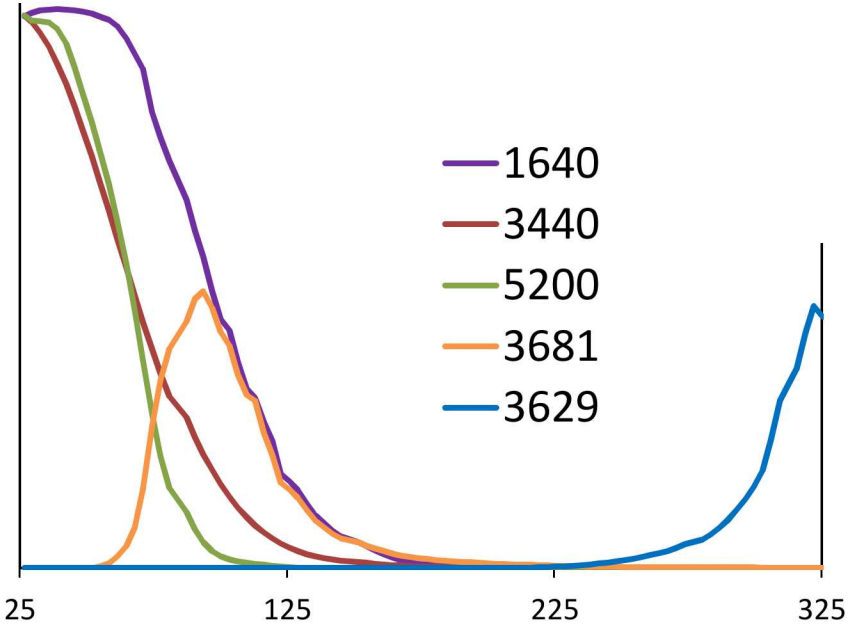

PDF

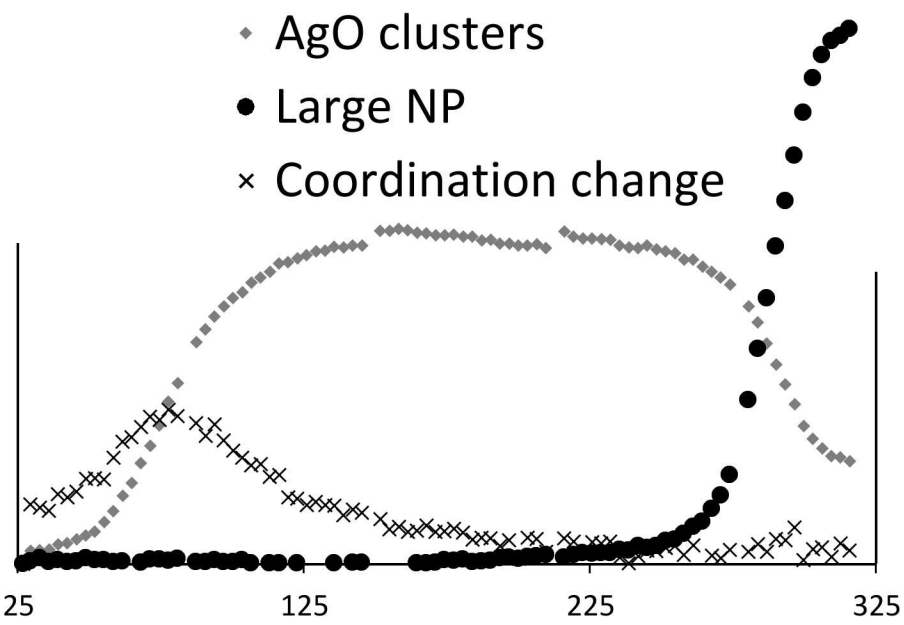

Thermal formation of small clusters (coinciding with H_2O loss)
In a reducing environmental, no formation of oxide

How does framework chemistry and/or geometry play a role in NP formation?

Comparison of
combined PDF & DRIFTS

Zeolites Y, A, MOR
in H_2 (reducing environment)
vs He (autoreduction/heat)

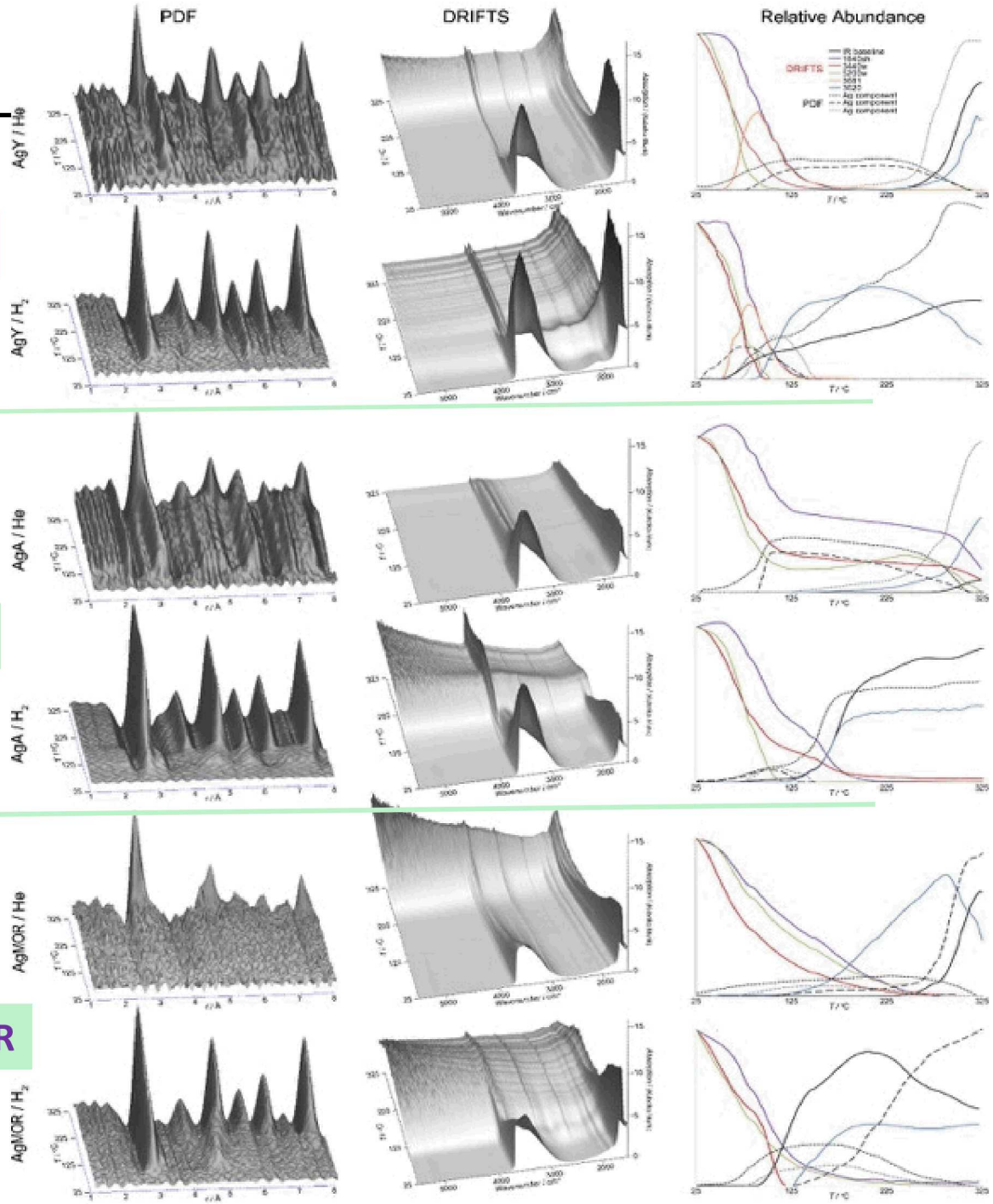

T. M. Nenoff, tmnenof@sandia.gov

R&D Area 3: Nanoporous Materials Membranes for Light Gas & Hydrocarbon Separations

H_2 Purification

Nature Mater., **2015**, *7*, 377; *Chem. Rev.* **2007**, *107*, 4078

MRS Bulletin, **2006**, 31(10), 735 (cover; Editor Nenoff)

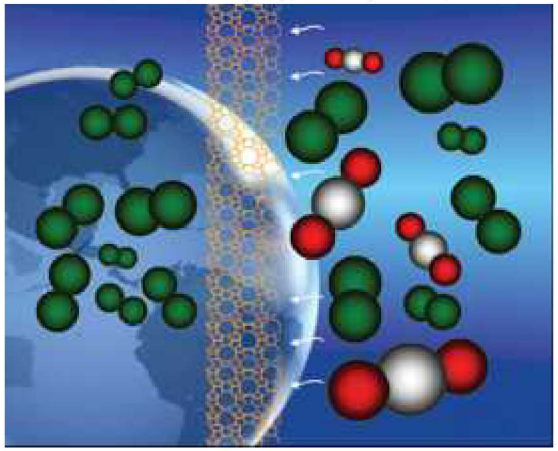

ZSM-5 Zeolite membrane for H_2 from CO_2 separations

Micro Meso Mater, **2003**, *66*, 181

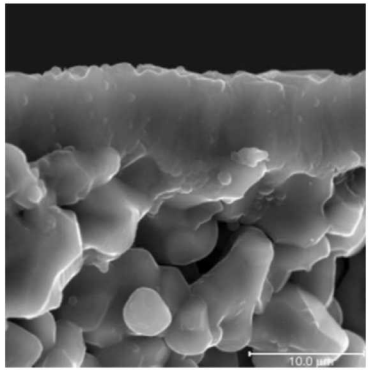

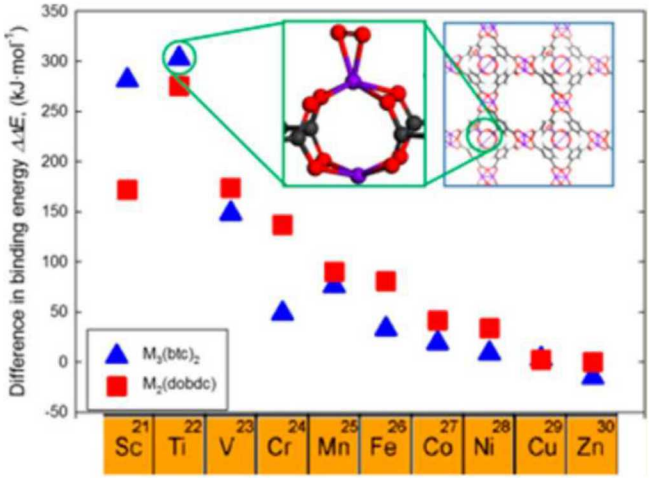

DFT/AIMD Designed Nanoporous Materials for O_2 from Air Separations for Energy Efficient Combustion

Chem. Mater. **2016**, 28(10), 3327

PCCP, **2016**, *18*, 11528

J. Phys. Chem. C, **2015**, *119*, 6556

Chem. Mater. **2015**, *27*(6), 2018

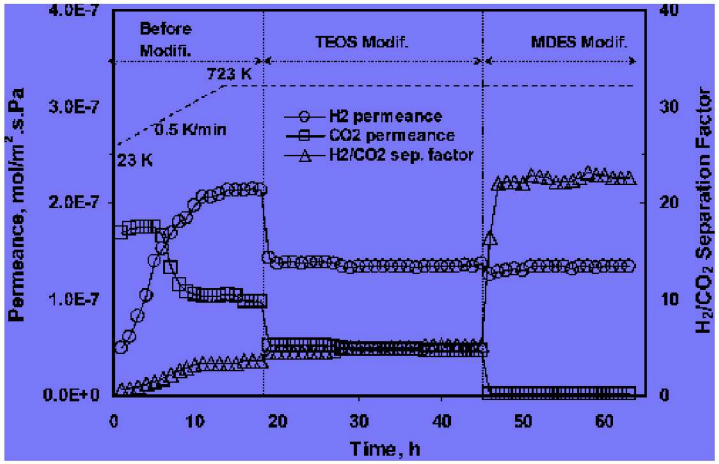

H_2 Purification from Syngas

Langmuir, **2009**, *25*(9), 4848

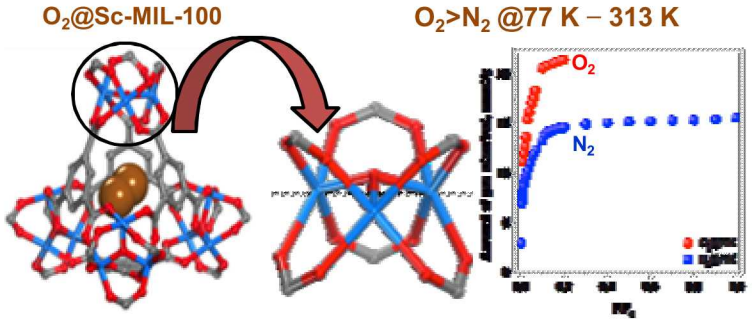

O_2/N_2 air separations with MOFs to Increase the Efficiency of the *ASU*

Basic Research directed to an *Energy Efficient Process* for Oxygen purification from air.
aka: how to increase the efficiency of the air separations unit (*ASU*)?

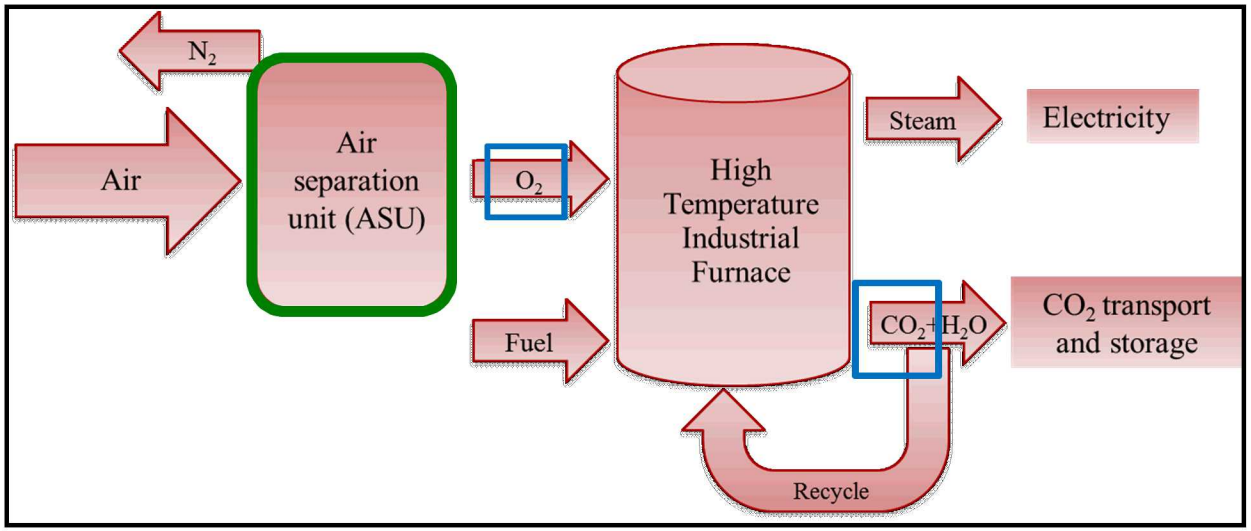

- Oxygen-enriched (oxy-fuel) combustion: burning the fossil fuel in an O_2 rich atmosphere results in a flue gas composed mainly of CO_2 (for capture) & water (little or no SO_X and NO_X emissions)
- The limiting factor of this technology is the efficiency of the cryogenic *ASU*, a costly and energy intensive process (primarily compression)
- Our study is focused on new highly selective materials (MOFs) to increase the efficiency of this separation process

Target O_2 Selective Separations Materials, DFT & Experiments

MOFs with coordinatively unsaturated metal centers are promising materials for O_2/N_2 separations

- Two prototypical MOFs from this category, $Cr_2(BTC)_3$[1], $Fe_2(DOBDC)$[2] both show preferential adsorption O_2 vs N_2
- Plane wave DFT calculations on periodic structures: Vienna Ab initio Simulation Package (*VASP*)
  - Binding geometries for side-on and bent O_2 and bent and linear geometries for N_2 were evaluated
  - Static binding energies for O_2 and N_2 at 0 K
- Use of DFT to determine M-O_2 vs M-N_2 binding energies

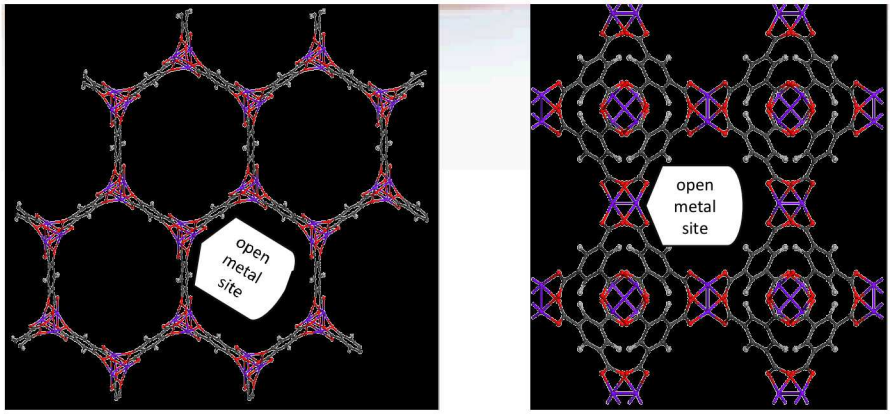

$M_2(dobdc)$ $M_3(btc)_2$

MOF metal sites = separate O_2/N_2 by differences in bonding & electronic properties

Plan wave density functional theory (DFT) calculations were performed on periodic structures of each MOF in the Vienna ab initio simulation package **(VASP)** with the Perdew-Burke-Ernzerhof **(PBE)** functional including dispersion corrections **(DFT-D2)**. Geometries were optimized and **static binding energies (ΔE_{O2}, ΔE_{N2})** were calculated by

$$\Delta E_{O2} = E_{MOF+O2} - E_{MOF} - E_{O2}$$

The **differences in binding energies ($\Delta\Delta$ E)** for oxygen and nitrogen were calculated by

$$\Delta\Delta E = -(\Delta E_{O2} - dE_{N2})$$

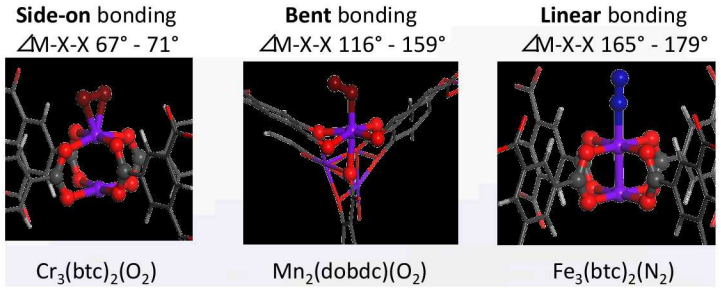

Attention Paid to Bonding Geometries

[1]*JACS* **2010**, *132*, 7856–7857; [2]*JACS* **2011,** *133*, 14814-14822

O_2 and N_2 Binding Energies Trends Across the First Row Transition Metal Series

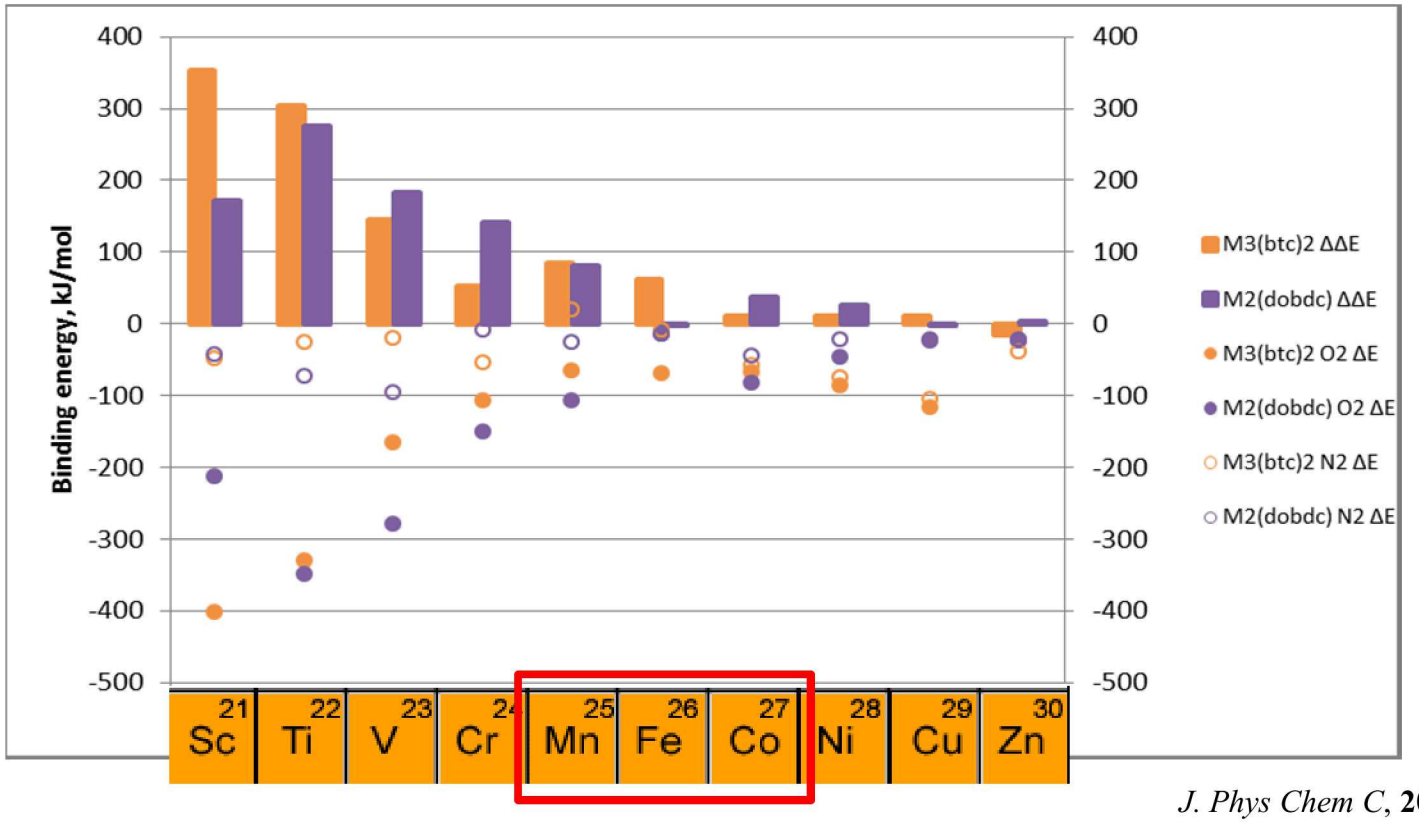

J. Phys Chem C, **2015**, *119*, 6556.

DFT predicts similar O_2 and N_2 binding to Mn, Fe, Co but with consistent stronger binding for O_2 to the metals

Postsynthetic Metal Ion Exchange to form Porous Mn-, Fe- and Co- Analogues of Cu-BTC

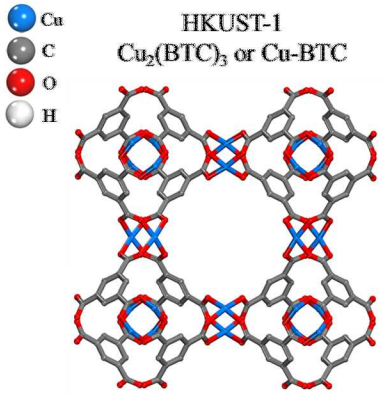

Chui, S. S. Y et.al Science **1999**, 283, 1148.

***M* = Mn, Fe, Co**

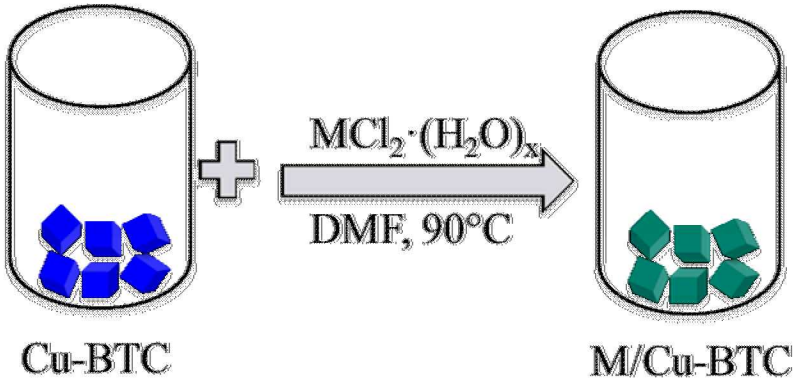

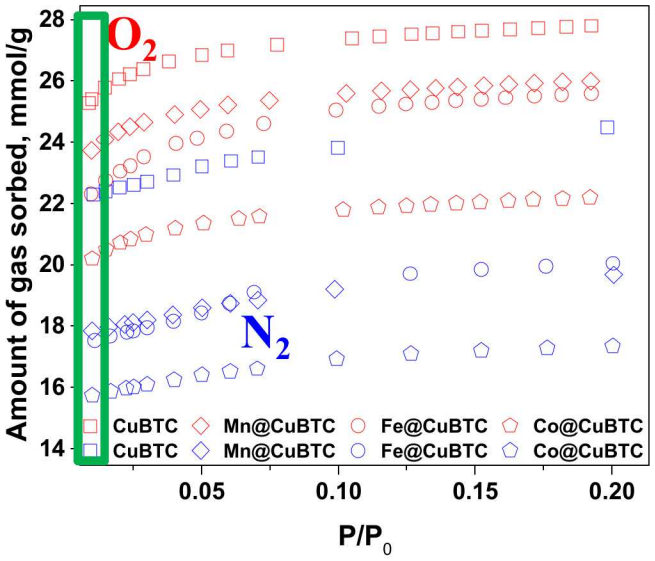

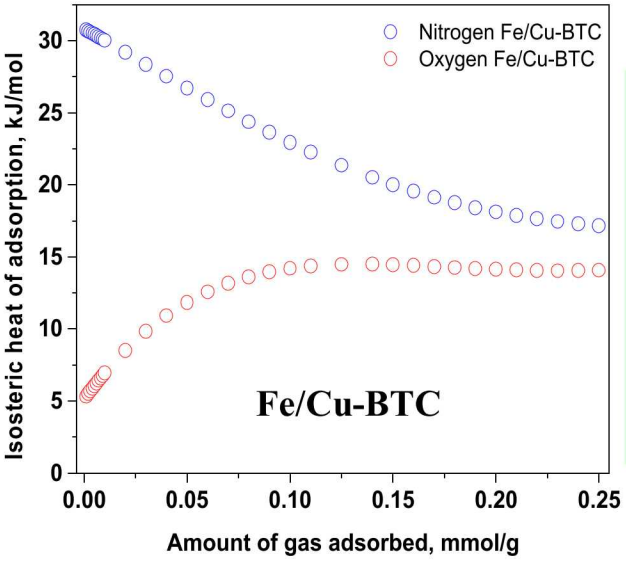

0 K *DFT binding energy*: Excellent prediction for 77K experiments,

Do not correlate as well with experimental data 273-298 K
- N_2 is preferred over O_2

Chem. Mater., **2015**, *27*(6), 2018.

AIMD Simulations with Temperature Considerations

M_2(dobdc) analogs

NVT ensemble: 27.5 ps, 0.5 fs timestep
PBE density functional with dispersion correction (PBE-D2),
PAW potentials for core electrons, spin polarization

Guests

	2 O_2 bound 4 O_2 unbound	2 N_2 bound 4 N_2 unbound
Single component	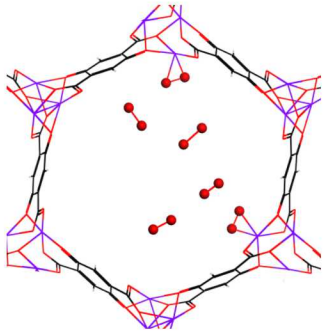	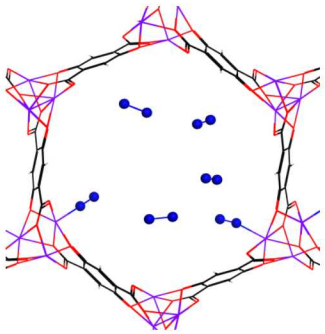
Mixed gas Competitive binding	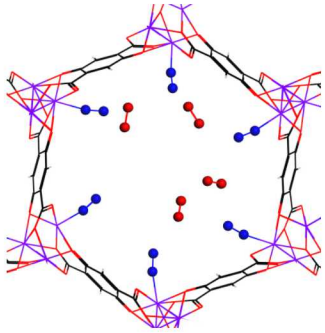	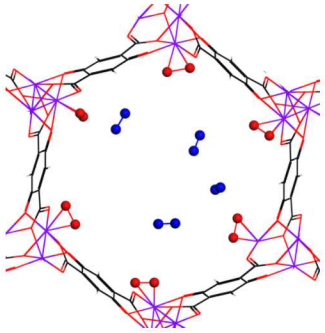
	6 N_2 bound 4 O_2 unbound	6 O_2 bound 4 N_2 unbound

Temperatures

201 K
258 K
298 K

Metals

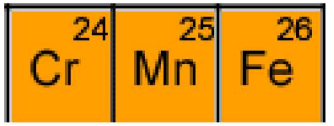

Red Sky Supercomputer
36 Simulations

3,800 processor-days each

http://hpc.sandia.gov/

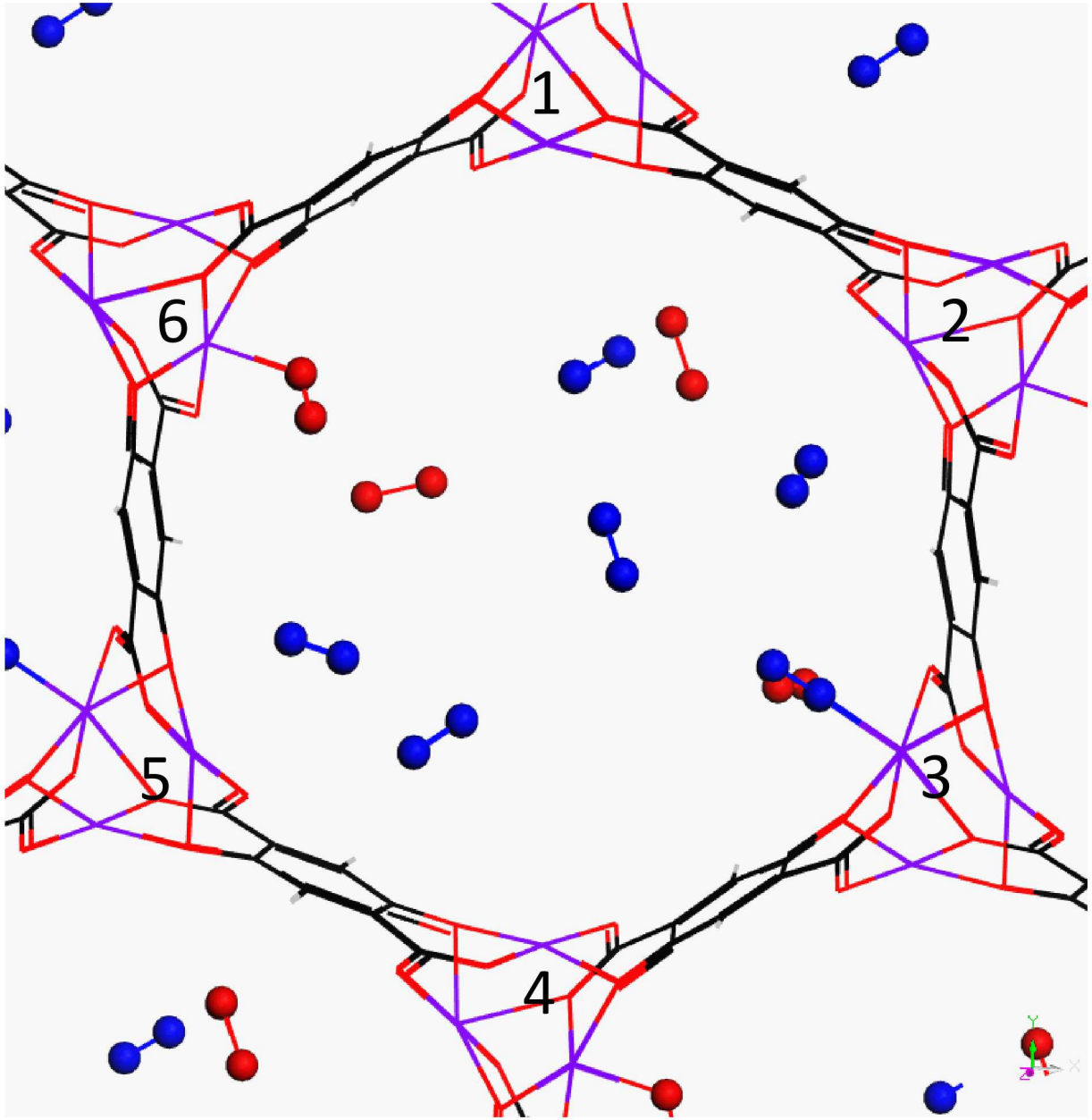

Cr_2(dobdc)
6 N_2 + 4 O_2
298 K

NVT
Time 2 ps – 15 ps

1 frame = 25 fs

- O_2 slow to bind, but once on metal center, binding holds
- N_2 rapid bind and release from metal centers
- O_2 long term binding is consistently 'bent'
- Selective for O_2

Gas Occupancy at Each Metal Site

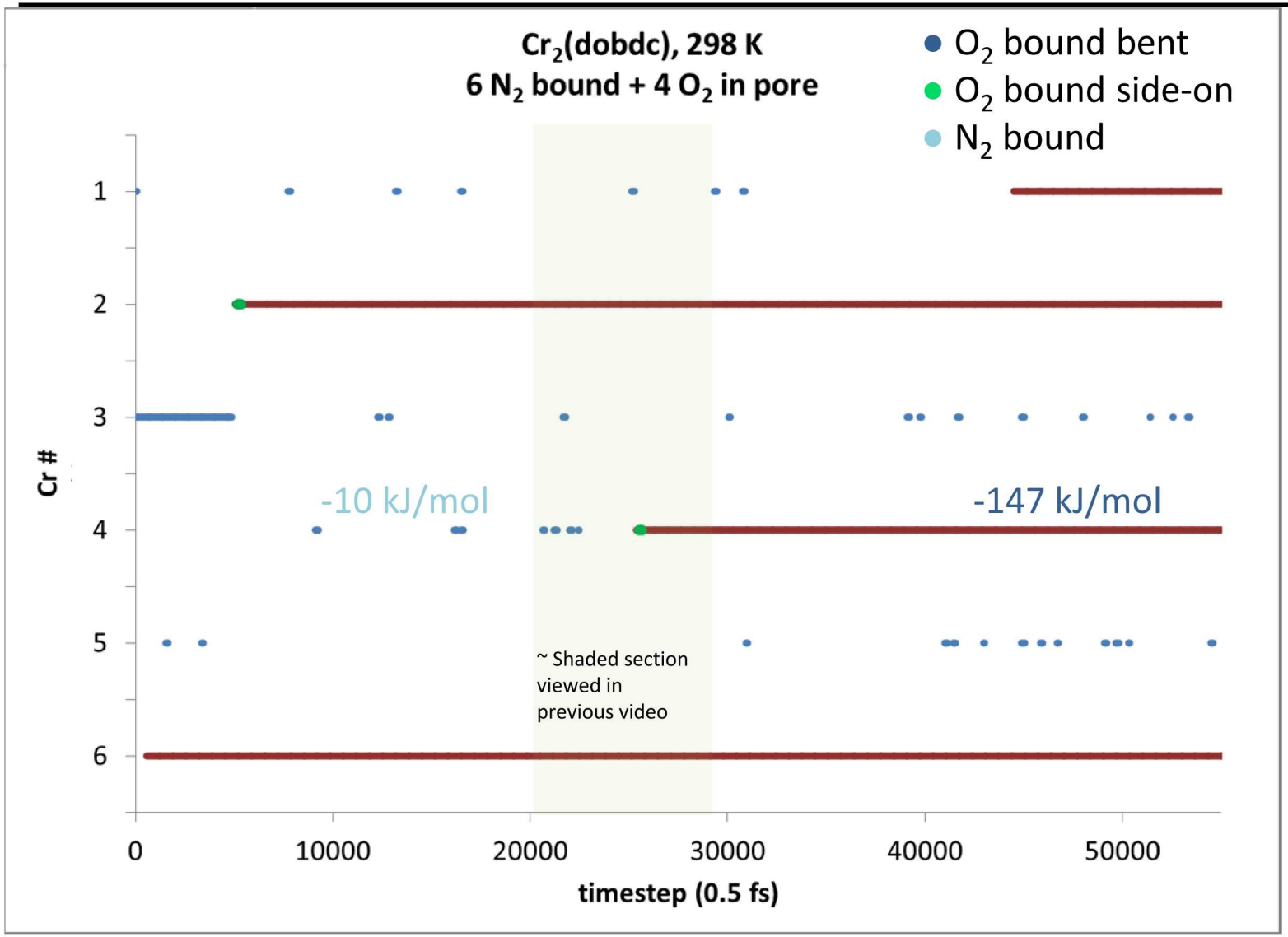

Gas Occupancy at Each Metal Site

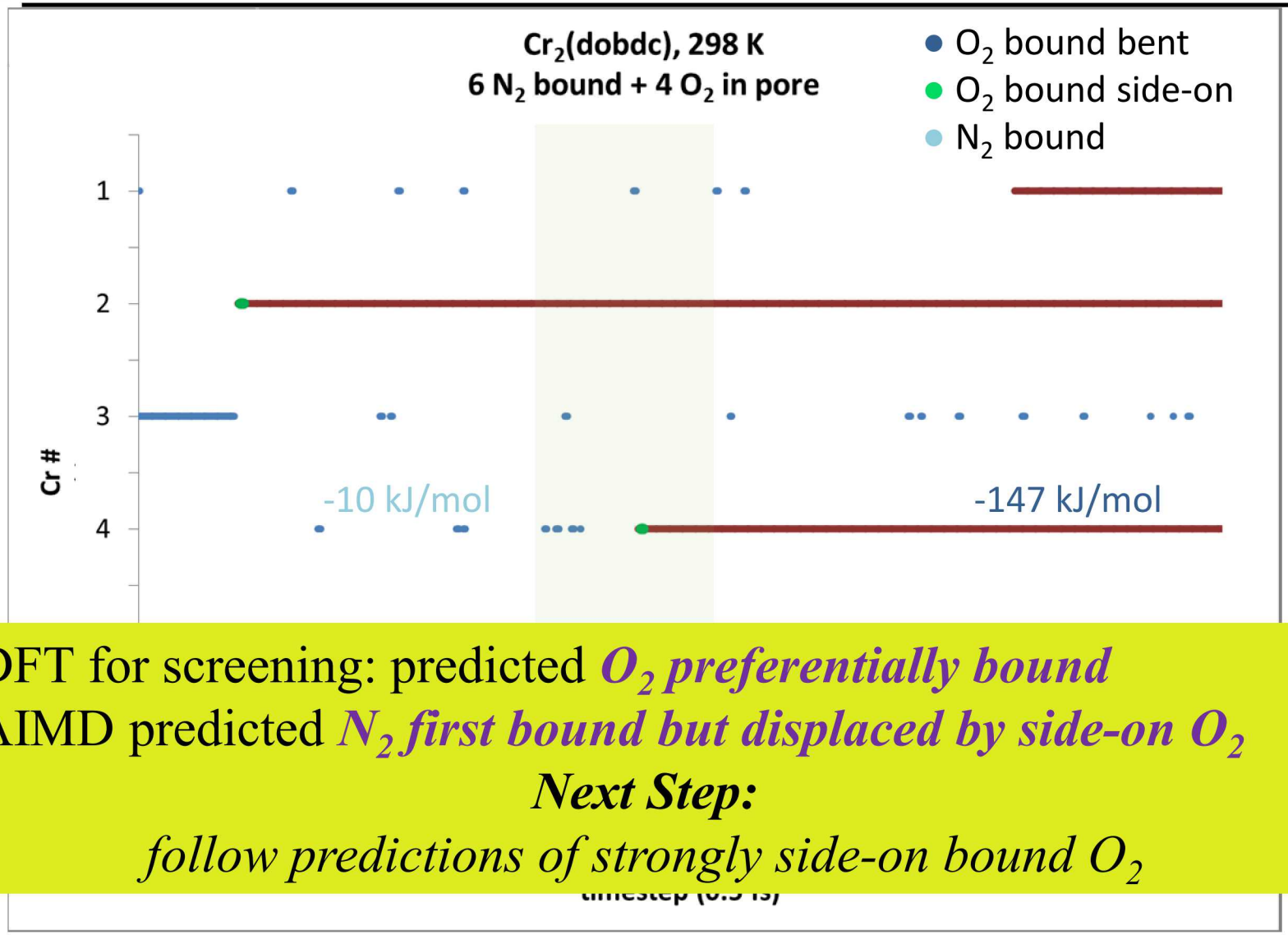

DFT for screening: predicted ***O_2 preferentially bound***

AIMD predicted ***N_2 first bound but displaced by side-on O_2***

Next Step:

follow predictions of strongly side-on bound O_2

Use of Strongest *Side-On Binding* Predictions

Sandia National Laboratories

Binding Energy Calculated as a Function of Metal Site

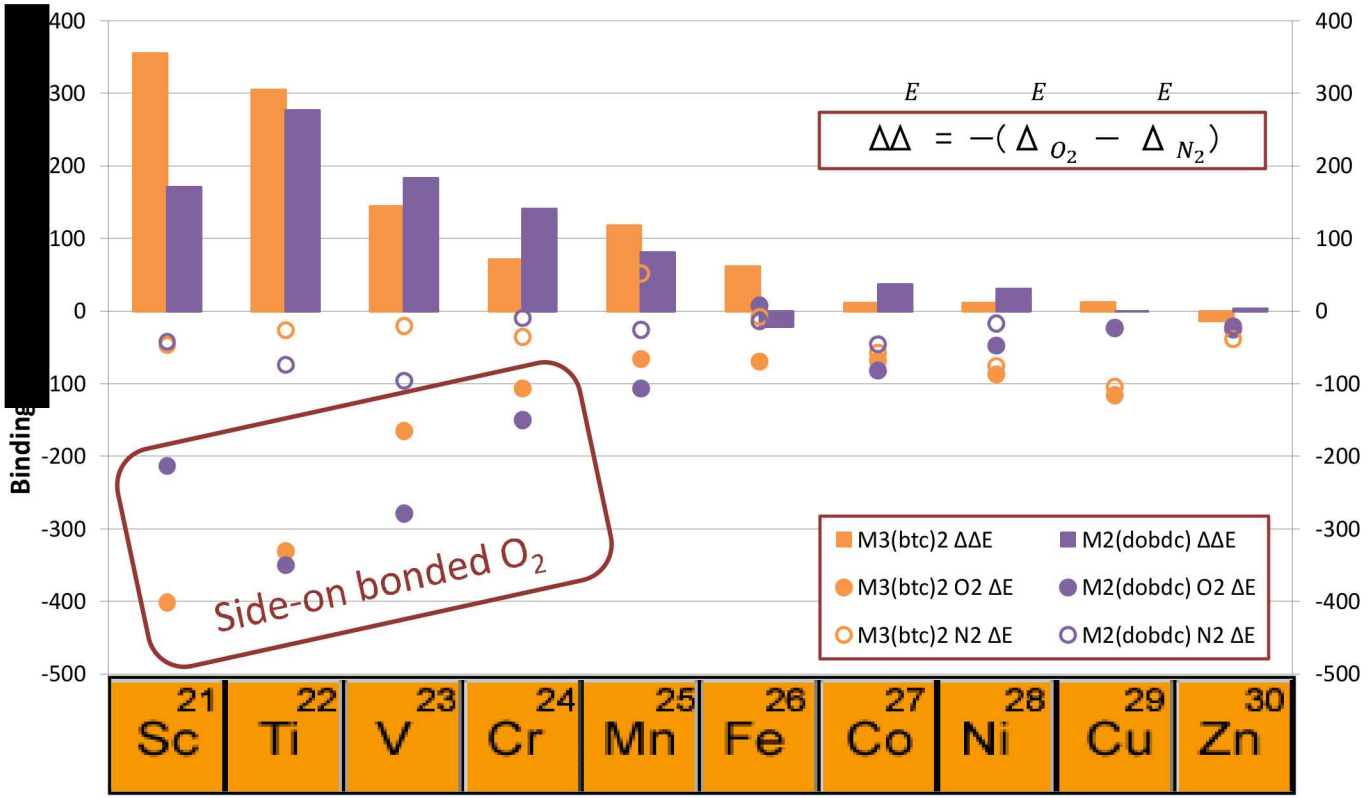

J. Phys Chem C, **2015**, *119*, 6556.

Inspired MOF Synthesis: Sc/BTC/DMF/HCl

Unique synthesis:

Mixed $Sc(NO_3)_3 \cdot xH_2O$ and 1,3,5–benzetricarboxylic acid in N,N'-dimethylformamide and HCl.

Heated to 373K overnight

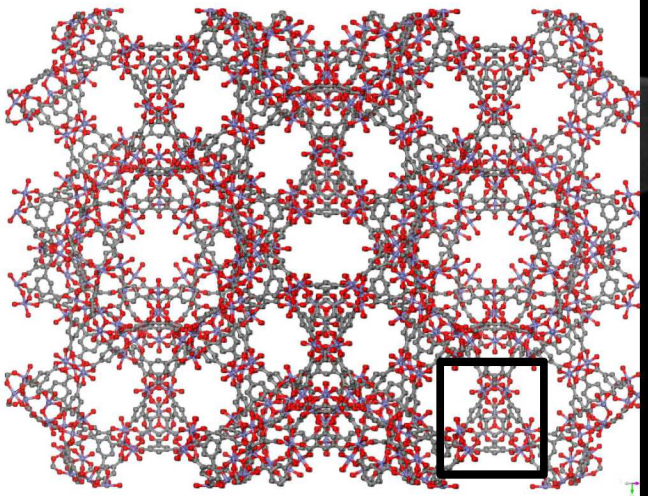

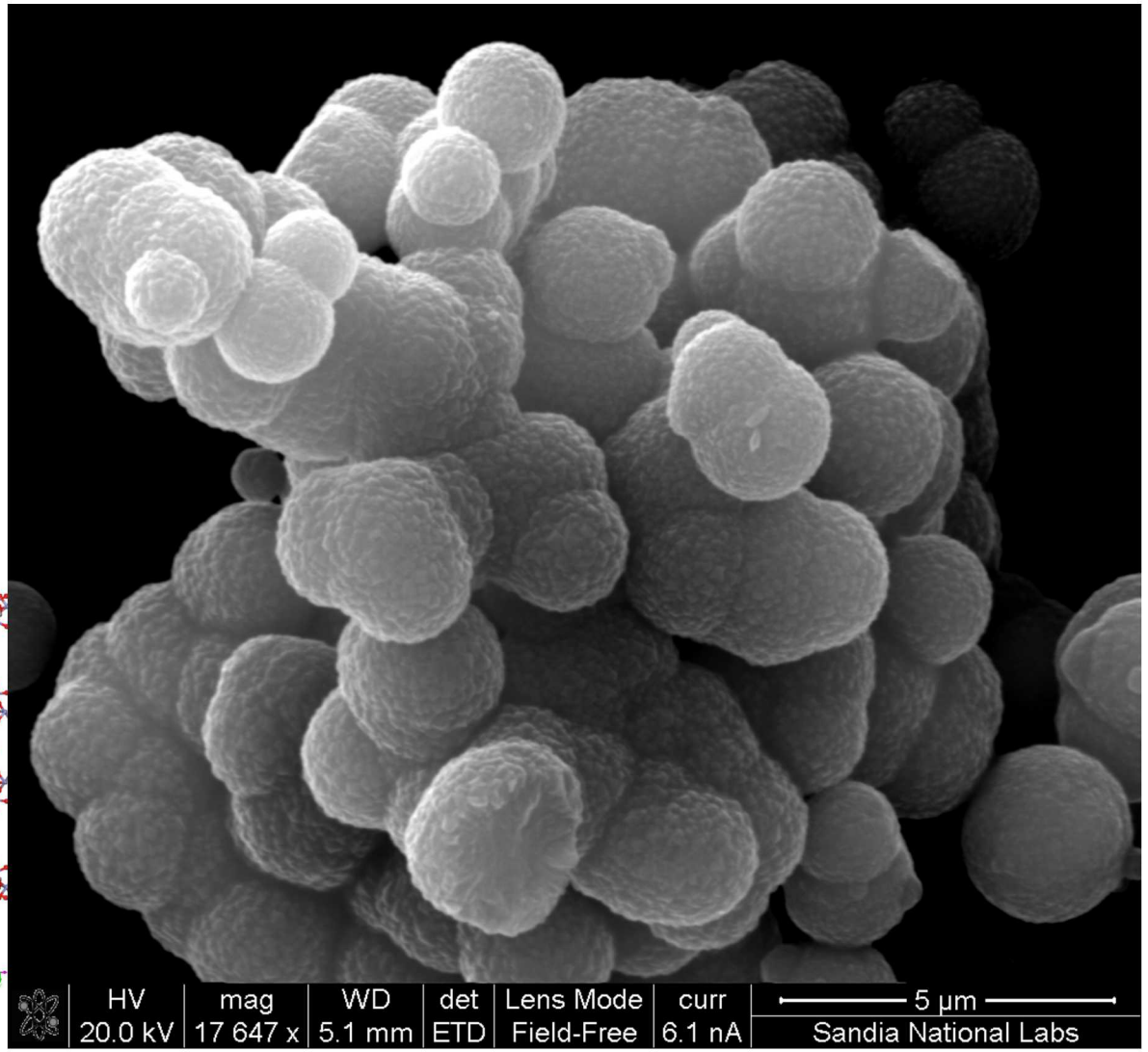

Chem. Mater. **2016**, 28(10), 3327-3336

Metal-Center has a role at 77K

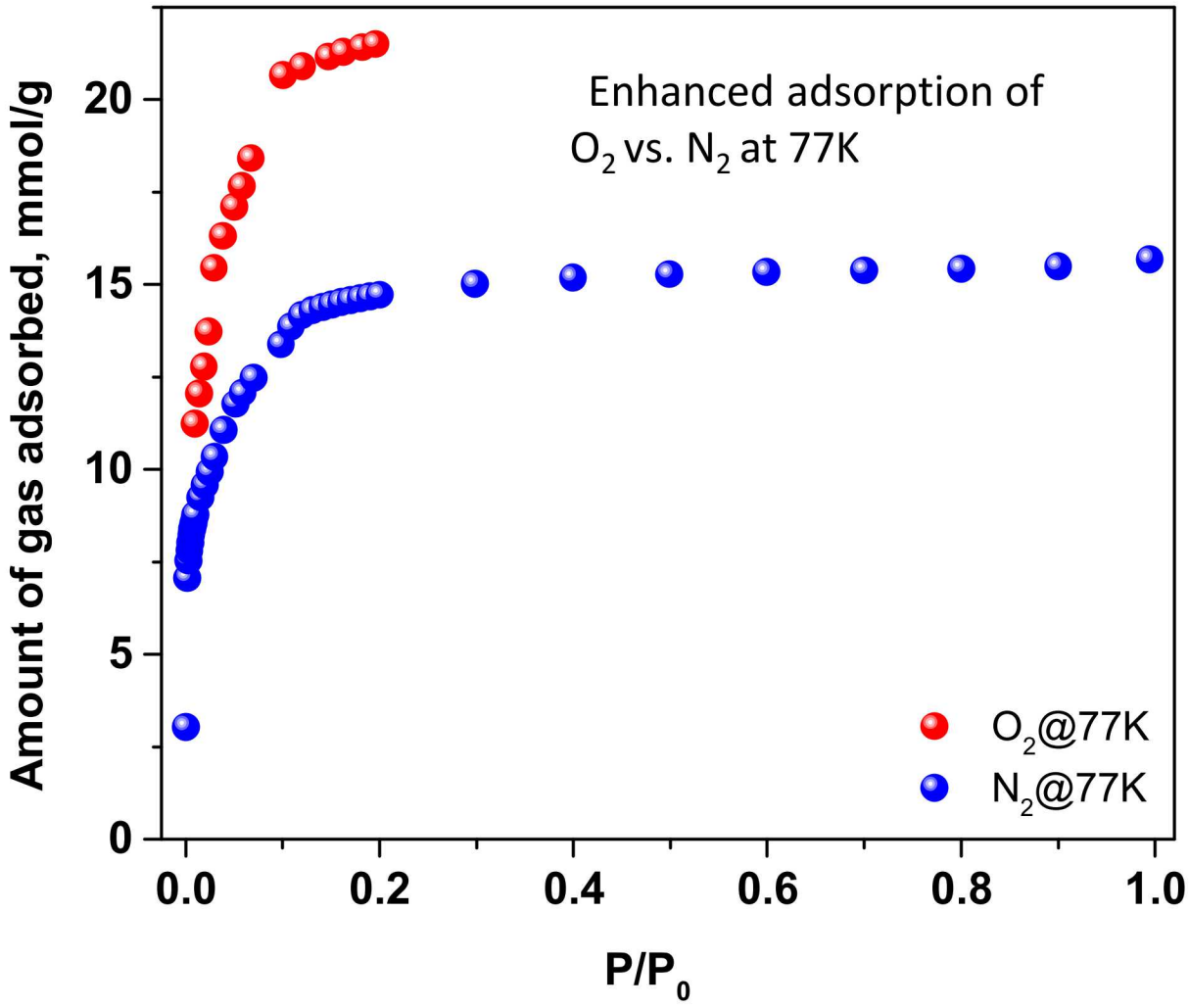

How does Sc-MIL-100 behave at more realistic operational temperatures?

ıhanced Quantity of O_2 vs N_2 Adsorbed le Temperature Range (at least to 313K)

Sandia National Laboratories

O_2 vs. N_2 @**258K**

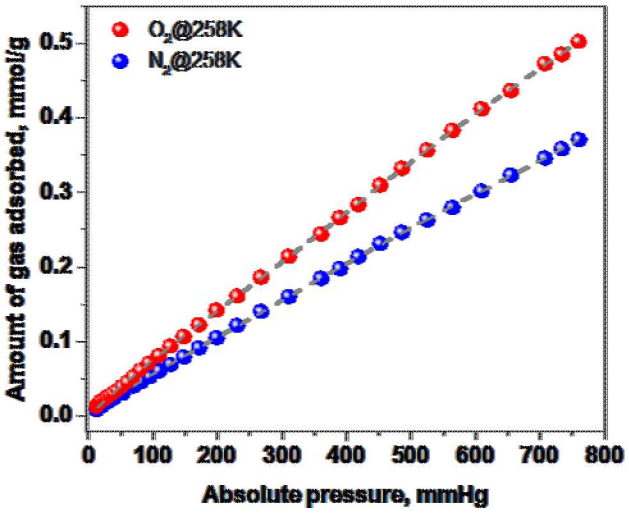

O_2 vs. N_2 @**298K**

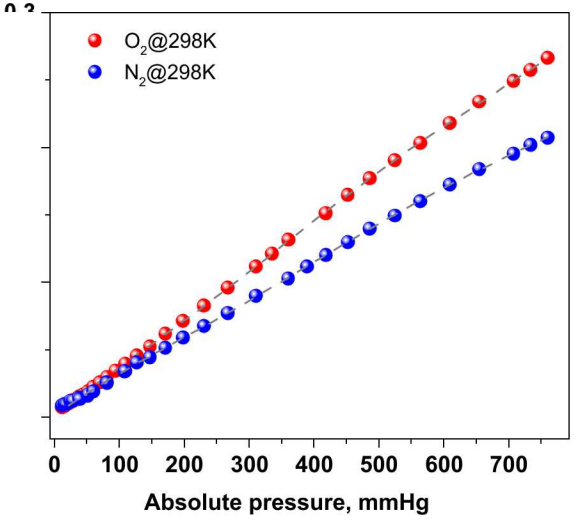

O_2 vs. N_2 @**313K**

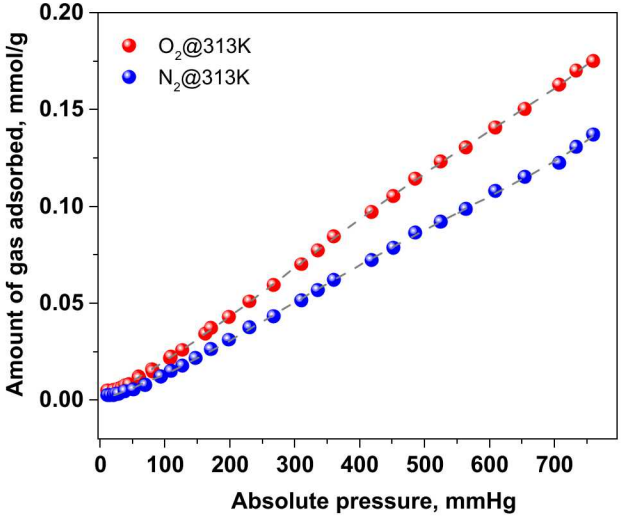

Isotherm trends mimic those predicted by GCMC

sosteric Heat of Adsorption (kJ/mol)
ding Energy for O_2 vs N_2

Qst derived from 258K, 298K and 313 K
Independent Virial Fit HOA

$$\ln P = \ln N + \frac{1}{T}\sum_{i=0}^{m} a_i N^i$$

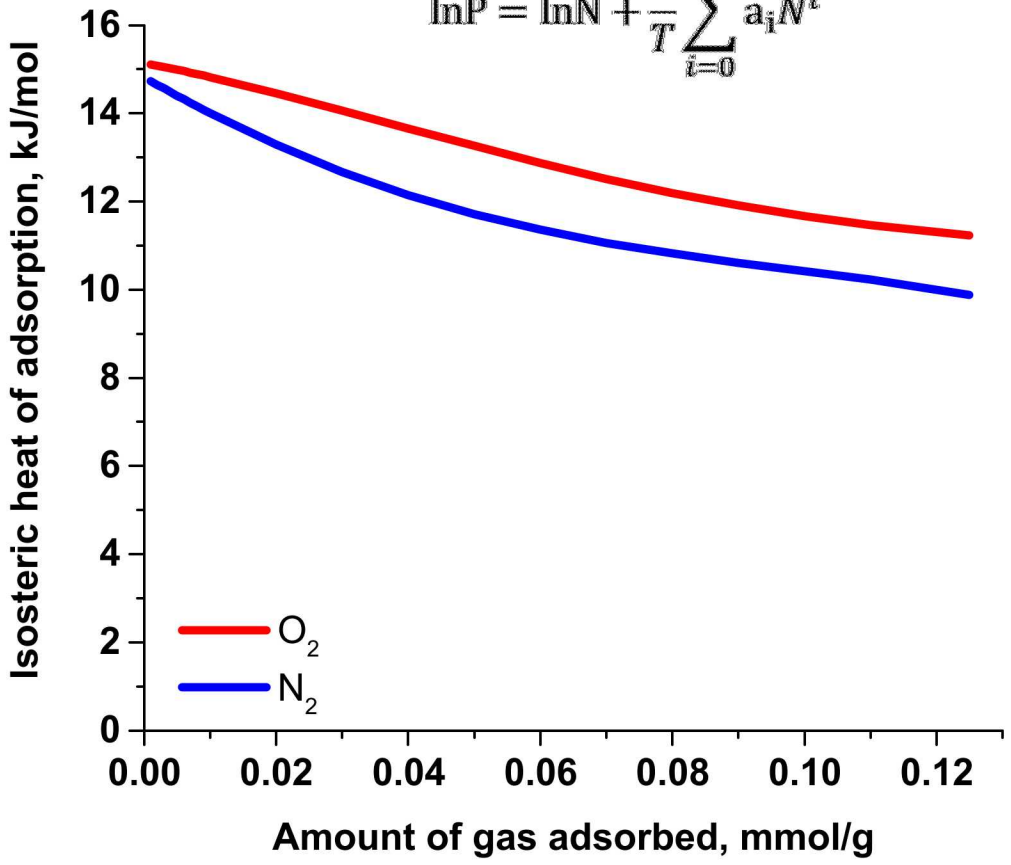

Sc-MIL-100 Performance

O_2 adsorption & Desorption over 10 cycles, 298 K, 1 atm

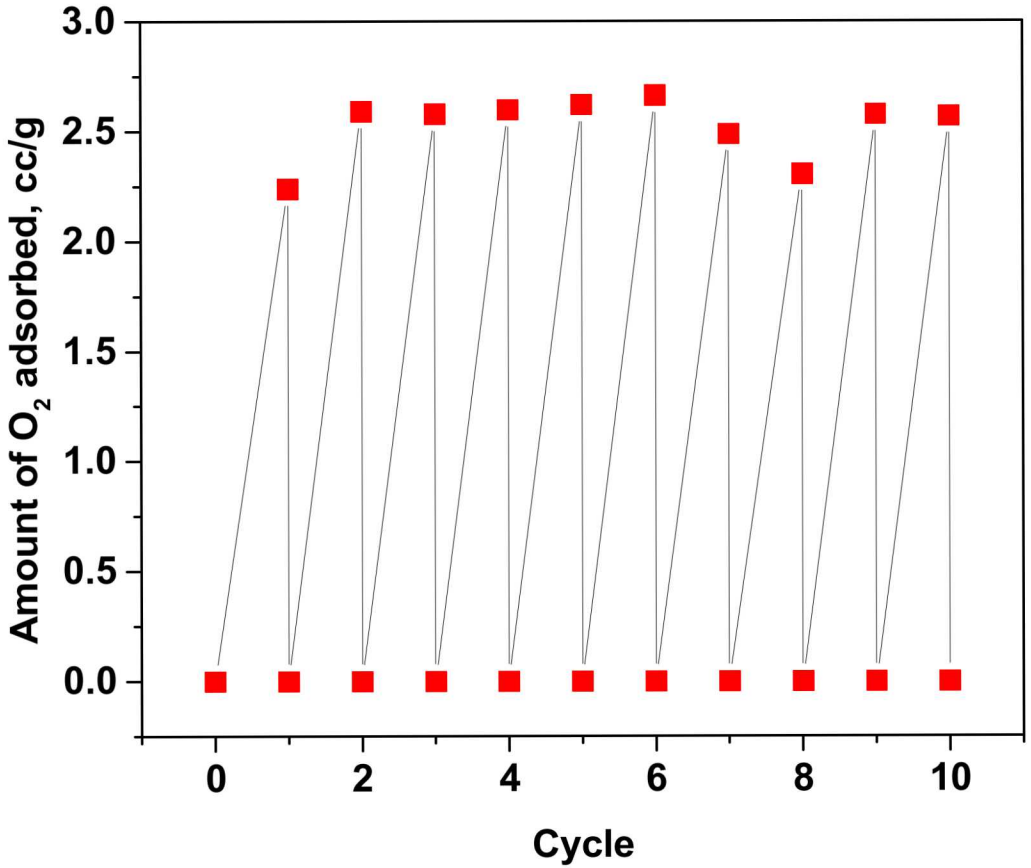

What about the structure is making Sc-MIL-100 O_2 strongly sorbing?

US provisional Patent 2019, licensed to NuMat and TDA Research 2019

Structure-Property Relationship
Understanding of Sc-MIL-100 O_2 Selectivity

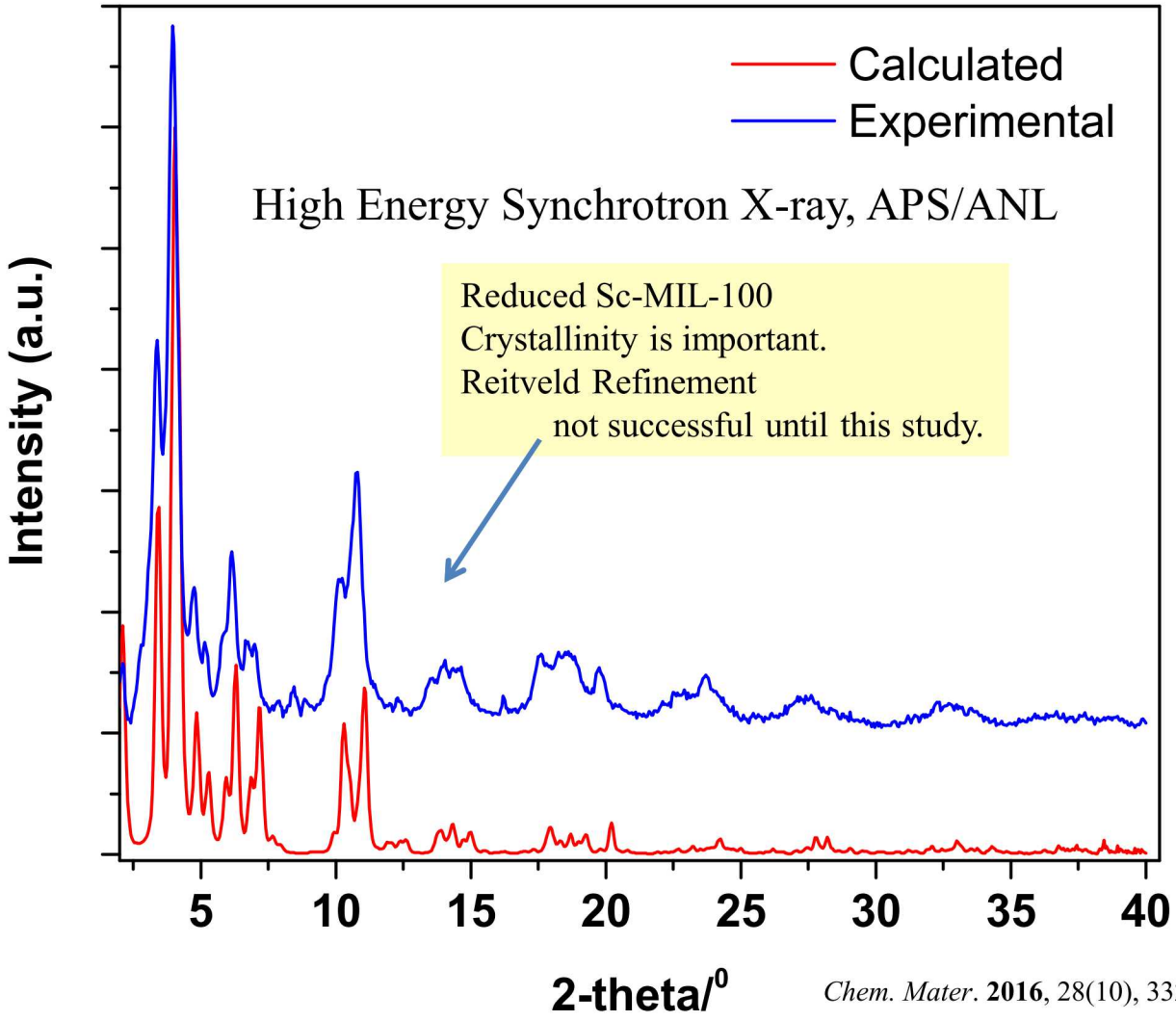

Chem. Mater. **2016**, 28(10), 3327.

Sc-MIL-100: Structure-Property relationship evaluated using Differential (d)- PDF

Sandia National Laboratories

d-Pair Distribution Function (d-PDF)

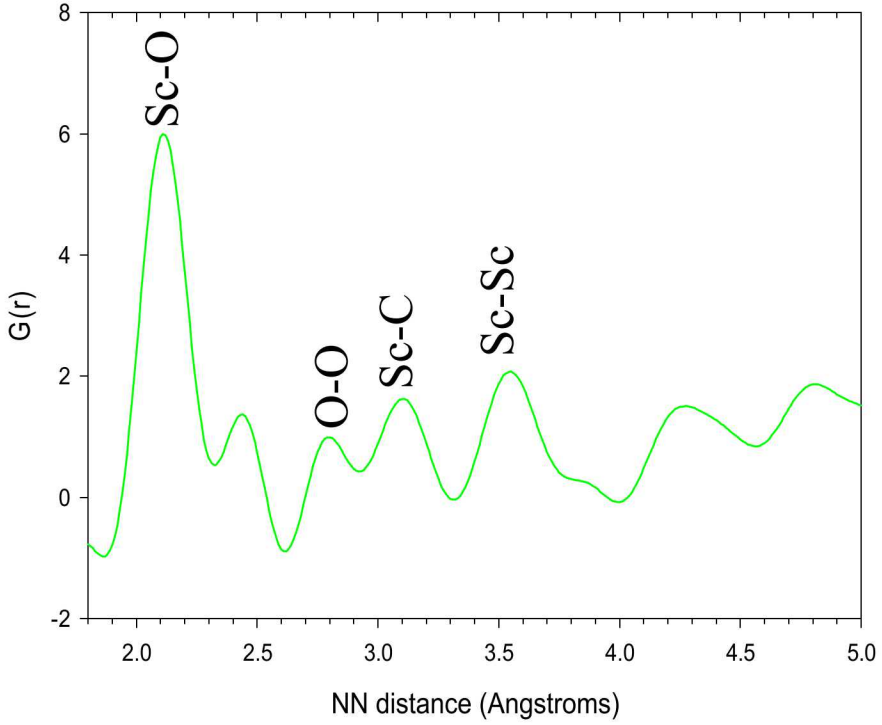

Peaks shifted to longer distances
Consistent with larger Sc incorporation
(vs. Cr-MIL-100)

d-PDF peak analysis

Bond	NN distance (Å)	Area	FWHM (Å)
Sc-O	**2.11**	**1.5**	**0.19**
O-O	2.81	0.3	0.22
Sc-C	3.08	0.8	0.26
Sc-Sc	3.53	0.5	0.24

- Oxo-centered trimers at nodes of MIL-100 framework inferred from M-O and M…M distances
- Narrow Sc-O peak = narrow Distribution of bond lengths
- Single M-O bond length (M-O(μ_3) or M-O (carboxylate)), suggests **M-O-M angle of 113°**
<< 120° of a planer trimer

Sc-MIL-100: Preferred O_2 sorption – Large Sc Distorts Cluster

Large size of Sc atom requires **out of plane distortion** in the ozo trimer of the O(μ3) atom.

Resultant "**puckering**" of trimer and "bending" of ligand is probable route for enhanced O_2 sorption / insertion in Sc-MIL-100

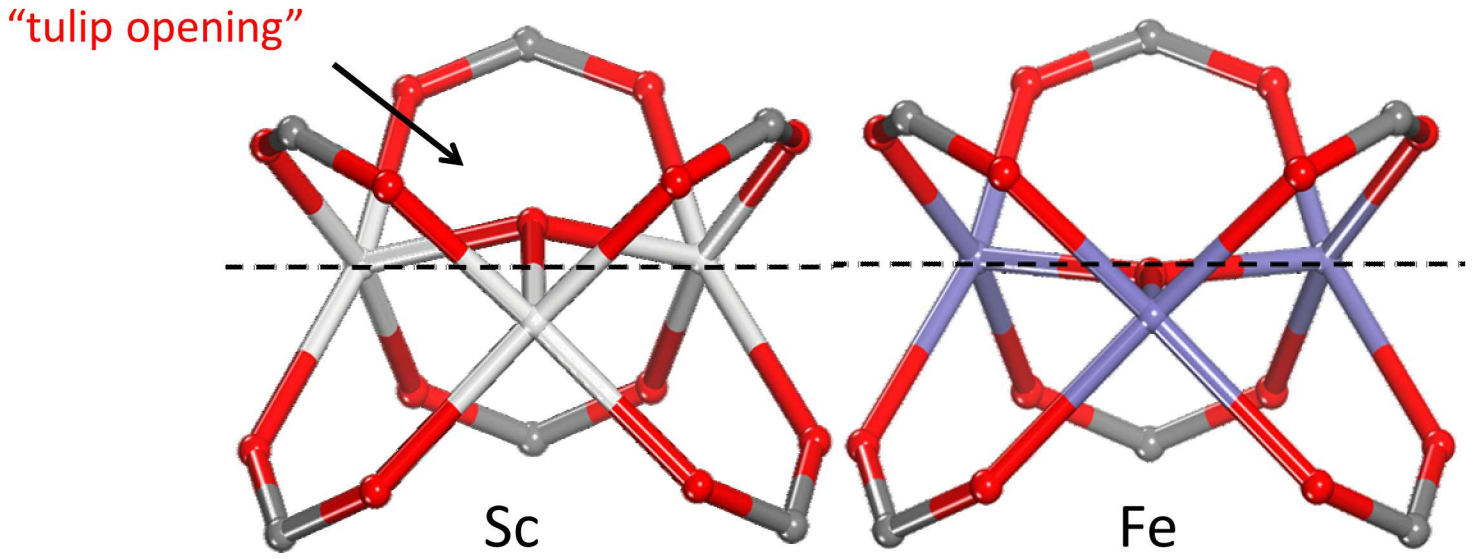

Rietveld refinement unit cell for Sc-MIL-100: a = 74.518(31) Å, R = 10.7%

Sc-MIL-100: Probable Sc-O binding sites

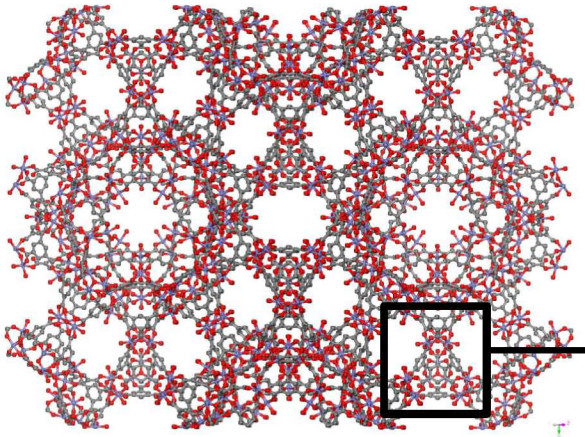

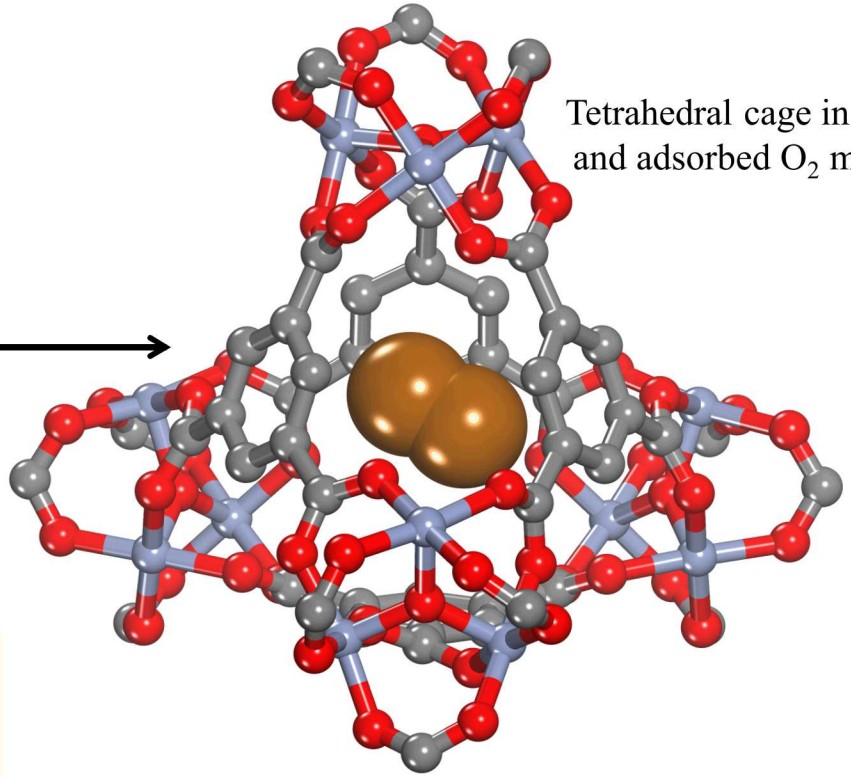

Tetrahedral cage in the MIL-100 framework and adsorbed O_2 molecule (large spheres).

GCMC-equilibrated configurations:
Cage and pore occupancy
as determined at 298K and 1 bar

P (bar)	Gas	# in Cage	# in Pore	Total
1	N_2	21	27	48
1	O_2	47	20	67

Example 4: Metal-Organic Framework Materials Photoluminescence Applications, low density, QY stability

SMOF-1: white light emitter

JACS, **2012**, *134*, 3983

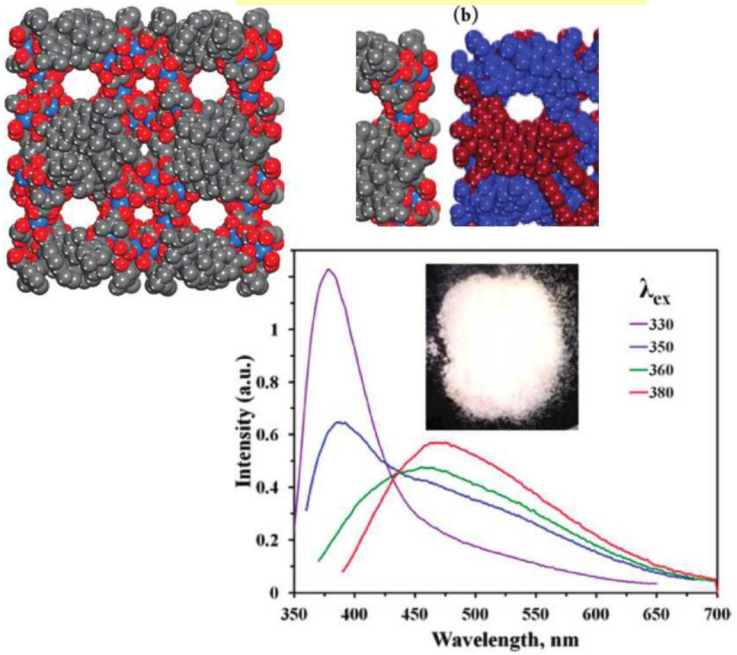

MOF tuned to "warm" white light

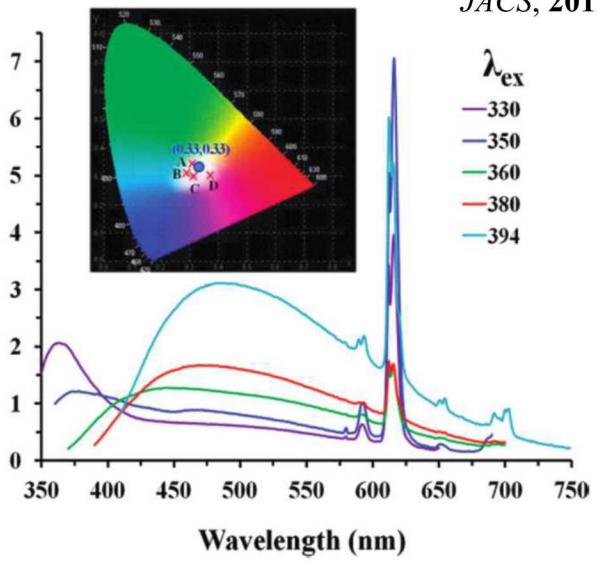

Chem. Mater. **2014**, *26*, 2943

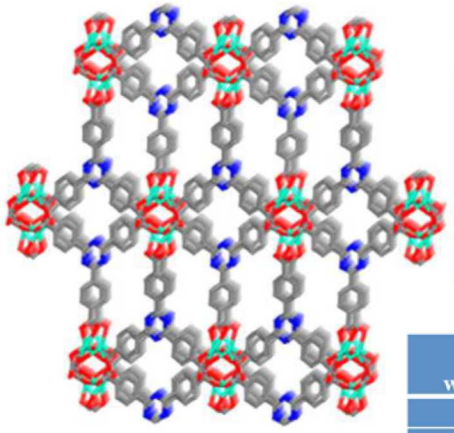

SMOF-7: red light emitter, high quantum yield with thermal stability for OLED applications

Excitation wavelength, nm	25°C	100°C	150°C
340	46%	50%	48%
394	22%	22.3%	19%

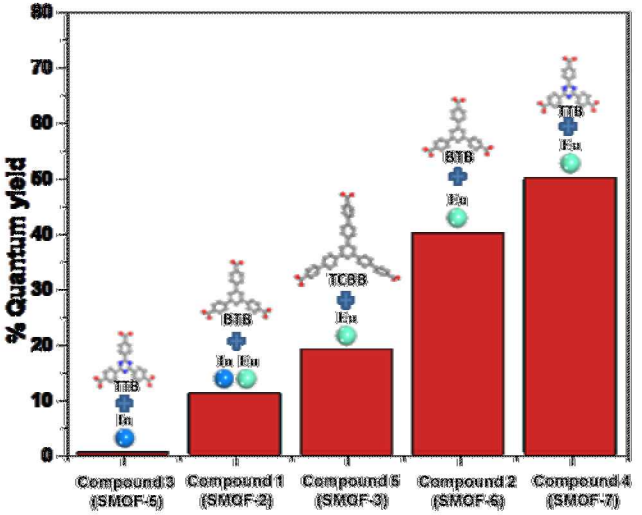

Example 4: Rare Earth – MOFs
PL & Acid Gas Durability

Team of modelers, synthesis and characterization of zeolites and MOFs with caustic gases

Goal: Investigate the structure-property relationship in a series of isostructural rare-earth MOF materials platform for NOx adsorption

- Explore scaleup synthesis methods for range of characterization (Grace Vincent, SNL/UNM undergrad)
- Probe the effect of metal ion identity in the adsorption/selectivity for NOx (Dorina Sava Gallis (SNL))
- Preliminary testing in house at SNL; Complementary modeling work for Jon Vogel (SNL postdoc)
- Team with Ryan Lively (GeorgiaTech) for mixed gas testing and Katharine Page (ORNL) for characterization

Activities/Findings

- Preliminary tests indicate that the materials remain crystalline upon NOx exposure for 24 hrs
- XRD studies reveal noticeable peak shifts to the right in the higher two-theta region indicative of host-guest interactions
- Correlated and complimentary VASP modeling to describe MOF strength and acid gas binding energies.

$M_6(\mu_3\text{-}OH)_8(C_8H_4O_6)_5(C_2H_6O_6)_1(H_2O)_6{\cdot}24H_2O$
M= Eu, Nd, Yb, Y, Tb and tuned compositions of Nd/Yb

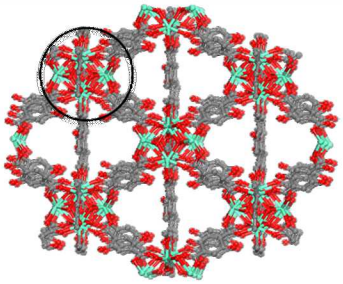

ACS Appl.Mater.Inter. **2017**, *9*, 22268.

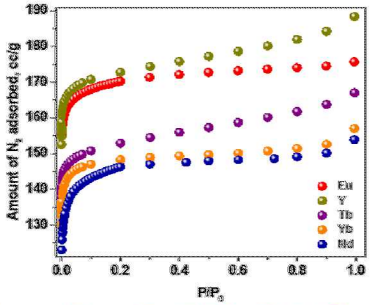

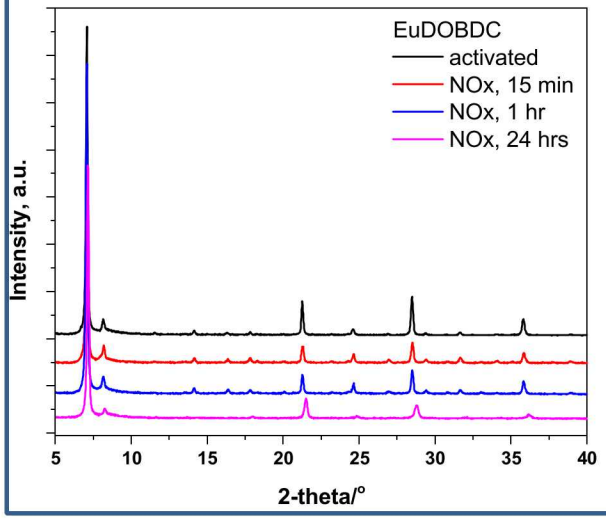

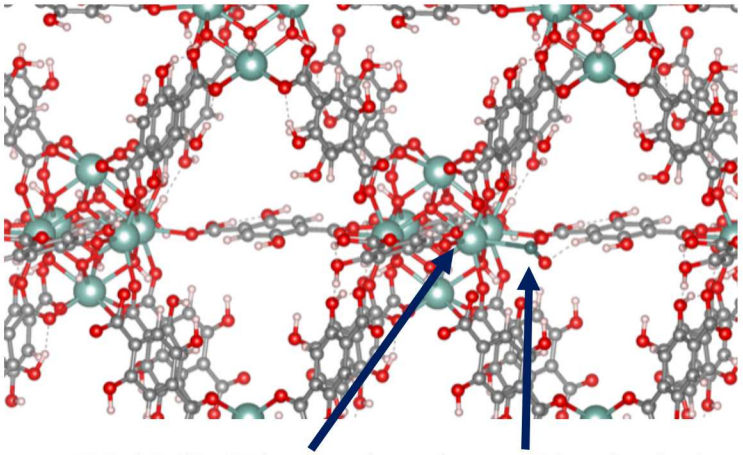

Y-DOBCD, Y hexanuclear cluster, NO_2 adsorbed

U.S. DEPARTMENT OF ENERGY | Office of Science | Georgia Institute of Technology | OAK RIDGE National Laboratory | Sandia National Laboratories | THE UNIVERSITY OF ALABAMA | LEHIGH UNIVERSITY | PENNSTATE | WISCONSIN | Washington University in St. Louis | UNCAGE ME

Example 5: Materials Synthesis of Topological Quantum Materials

Cu-$ZrTe_5$: Synthesis and topological properties.
Phys Rev Mater **2019**, in prep.

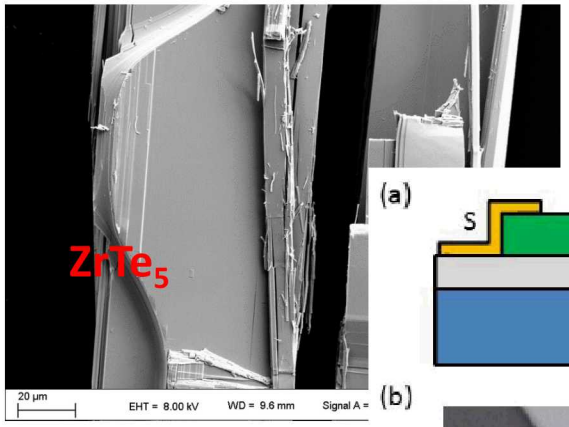

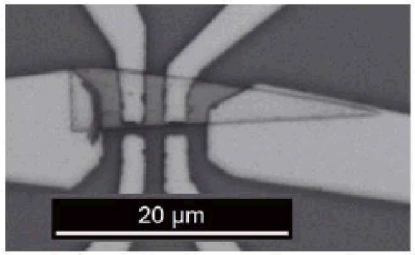

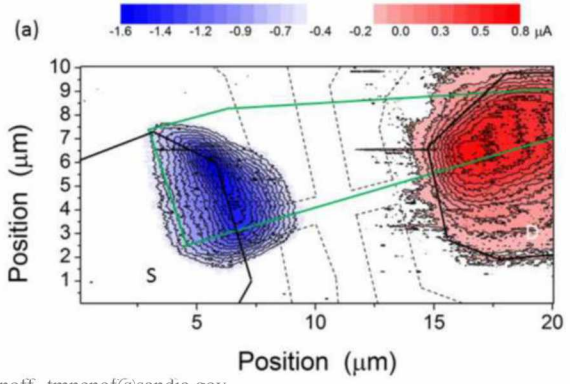

Invited Review & Cover:
Topological quantum materials for realizing Majorana quasiparticles.
Chem Mater **2019**, *31*(1), 26–51

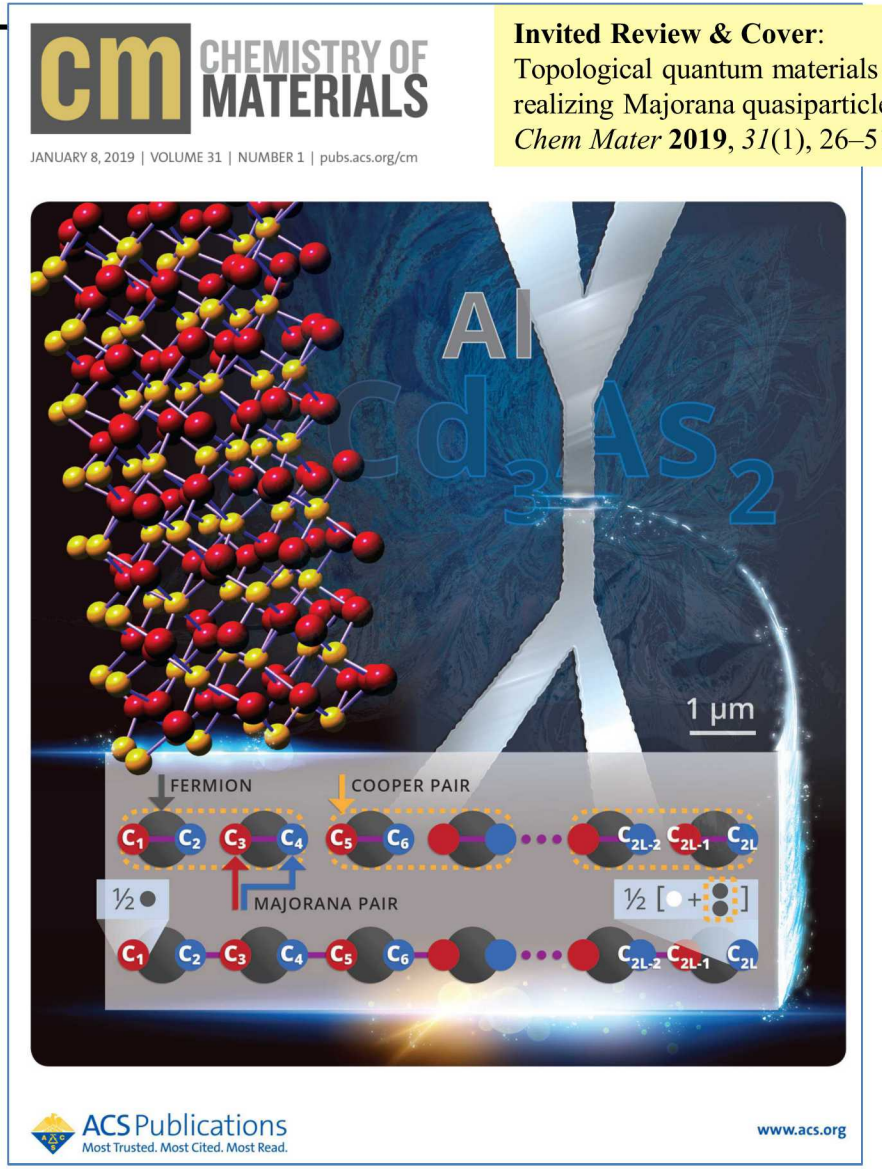

Superconducting Al (low temp) with the Cs_3As_2 (TQM) enables the p-wave superconductor, requirement for creating Majorana fermions

Conclusions

- Multidisciplinary teaming allows for in-depth understanding of materials structure-properties
- The collaborative use of DFT and AIMD modeling enables the materials design, and reactivity prediction, needed to understand the chemistry and reactivity inside nanopores
- STRONG collaboration of light source user facilities with materials synthesis and testing for structure-property relationship understandings.
- We are always looking for collaborations!!

Acknowledgements

For Projects Highlighted herein

Sandia National Labs:
- Leo Small
- Dorina Sava Gallis
- Mark A. Rodriguez
- David X. Rademacher
- Lauren Rohwer
- Grace Vincent
- Jon Vogel

Stonybrook University:
- Karena W. Chapman
- Peter Chupas

Univ Idaho:
- Haiyan Zhao

ORNL/SNS:
- Katharine Page
- Luke L. Daemon

Funding Agencies:
- SNL LDRD
- DOE/NE - Fuel Cycle
- DOE/BES/EFRC- *UNCAGE-ME*
- DOE/SBIR

Sandia National Labs
Albuquerque, New Mexico

Questions? / Thank you

Pair Distribution Function (PDF) Analysis:
To see what is happening inside the pores

Use of high energy synchrotron:
high energy X-rays and large area detectors key to structure resolution of heavier elements such as *Silver*

The PDF, ***G(r)****,* is related to the ***probability*** of finding an atom at a distance ***r*** from a reference atom.
It is the Fourier transform of the total structure factor, ***S(Q)***.

$$\boldsymbol{G(r)} = 4\pi r\,\rho_0[\boldsymbol{g(r)}\text{-}1] = (2/\pi)\int Q[\boldsymbol{S(Q)} - 1]\sin(Qr)\mathrm{d}Q$$

probability — structure factor

The structure factor, ***S(Q)***, is related to coherent part of the diffraction intensity

$$\boldsymbol{S(Q)} = 1 + [\boldsymbol{I^{coh}(Q)} - \sum c_i|f_i(Q)|^2]/\ |\sum c_i f_i(Q)|^2$$

diffraction intensity (corrected)

Apply corrections for background, absorption, Compton & multiple scattering

PDF Provides Insight Into Short Range Structural Order

- a weighted histogram of ALL atom-atom distances

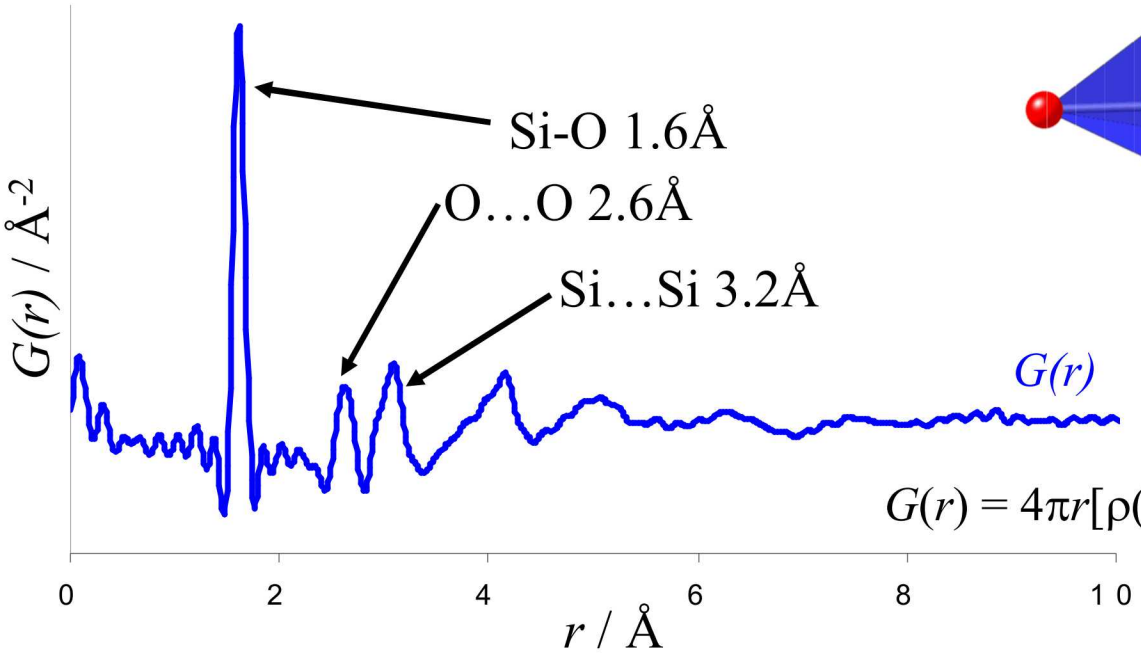

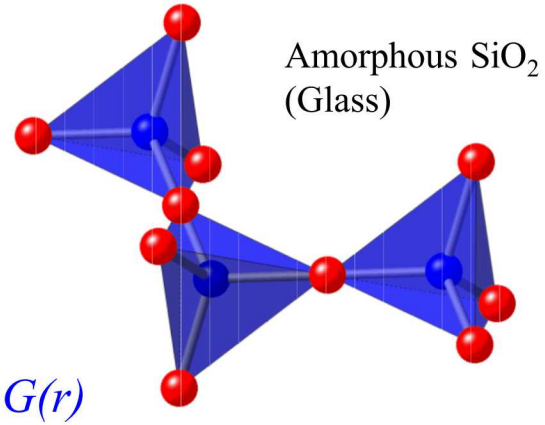

Peak position ⟷ Bond length / distance
Peak area ⟷ Coordination #, scattering intensity
Peak width ⟷ Disorder, bond angle distribution
Peak r_{max} ⟷ Particle size, coherence

→ **Structural Modeling**

Application to Zeolites to Examine Short Range Interactions of Guests in Pores